

Multimodal Locomotion of Soft Robots

Zihao Yuan, Huangwei Ji, Kai Huang, Feifei Chen,* and Guoying Gu*

Inspired by organisms that utilize multimodal locomotion strategies to adapt to diverse environments, the development of analogous capabilities in soft robots has garnered growing attention. This review comprehensively surveys recent advances in multimodal locomotion within soft robotics. Typical locomotion modes are summarized and categorized. Furthermore, the underlying mechanisms enabling multimodal locomotion, encompassing both the integration of distinct locomotion modes and transitions between them, are discussed in detail and classified into three primary categories: active control-based, reconfiguration-based, and environment-responsive strategies. Leveraging these mechanisms, soft robots demonstrate enhanced adaptability for applications such as cross-domain transition, surface adaptation, and obstacle negotiation. Finally, key challenges in advancing the capabilities of multimodal locomotion to address real-world applications are discussed.

integrated multimodal capabilities for deployment in diverse and unstructured scenarios (Figure 1), bridging soft robots closer to real-world applicability.

The rising interest in soft locomotive robots has led to a surge in studies aimed at characterizing and summarizing their capabilities. However, to the best of our knowledge, most existing reviews focus on an individual locomotion mode^[10–12] or present various modes in isolated contexts.^[13–15] Although recent reviews have begun to discuss multimodal or multi-environment locomotion of soft robots,^[16,17] a systematic analysis of the underlying mechanisms that enable mode transitions in response to environmental changes is still lacking. Deeper exploration of these mechanisms is essential for

unlocking the full potential of soft robots toward practical application scenarios.

In this review, we provide a comprehensive overview of recent advances in multimodal locomotion of soft robots. We first summarize and categorize eight typical locomotion modes. Subsequently, we delve into the underlying mechanisms that enable transitions between these modes, classifying them into three primary categories: active control-based, reconfiguration-based, and environment-responsive strategies. We then highlight how multimodal locomotion enhances adaptability in diverse scenarios such as cross-domain transition, surface adaptation, and obstacle negotiation. Finally, we discuss key challenges and propose future research directions concerning the efficient generation of multiple locomotion modes and their seamless transition, sensing and control, system integration, and decision-making toward real-world applications of multimodal soft robots.

1. Introduction


Throughout evolution, organisms in nature have developed sophisticated multimodal locomotion strategies to adapt to diverse environments.^[1] Many species switch between distinct gaits to navigate complex terrains or evade threats. For instance, octopuses transition from crawling with arms to jet propulsion for escape. Traditional rigid robots, constrained by fixed architectures, struggle to replicate such capabilities. Soft robotics, leveraging lightweight, compliant, and flexible materials, offers new possibilities.^[2–4] While early soft robots often exhibit only a single locomotion mode,^[5–9] limiting their utility in unstructured environments, recent years have witnessed growing attention toward developing multimodal locomotion in soft robots. This signifies a shift from single-mode operation in structured settings toward

Z. Yuan, H. Ji, K. Huang, F. Chen, G. Gu
Robotics Institute and State Key Laboratory of Mechanical System and Vibration

School of Mechanical Engineering
Shanghai Jiao Tong University
Shanghai 200240, China

E-mail: ffchen@sjtu.edu.cn; guguoying@sjtu.edu.cn

F. Chen, G. Gu
Shanghai Key Laboratory of Intelligent Robotics
Shanghai Jiao Tong University
Shanghai 200240, China

 The ORCID identification number(s) for the author(s) of this article can be found under <https://doi.org/10.1002/aisy.202500782>.

© 2025 The Author(s). Advanced Intelligent Systems published by Wiley-VCH GmbH. This is an open access article under the terms of the Creative Commons Attribution License, which permits use, distribution and reproduction in any medium, provided the original work is properly cited.

DOI: 10.1002/aisy.202500782

2. Locomotion Modes

Soft robots leverage inherent material compliance to achieve distinctive locomotion capabilities. Through ingenious structural design and actuation strategies, researchers have successfully replicated diverse fundamental locomotion modes observed in nature. These modes form the foundation for constructing more complex and adaptable multimodal locomotion. This section categorizes fundamental locomotion modes in soft robotics, thereby establishing a conceptual basis for subsequent discussions on multimodal locomotion (Figure 2). For reference, a comparative summary of these representative locomotion modes is provided in Table 1, encompassing key metrics such as actuation method,

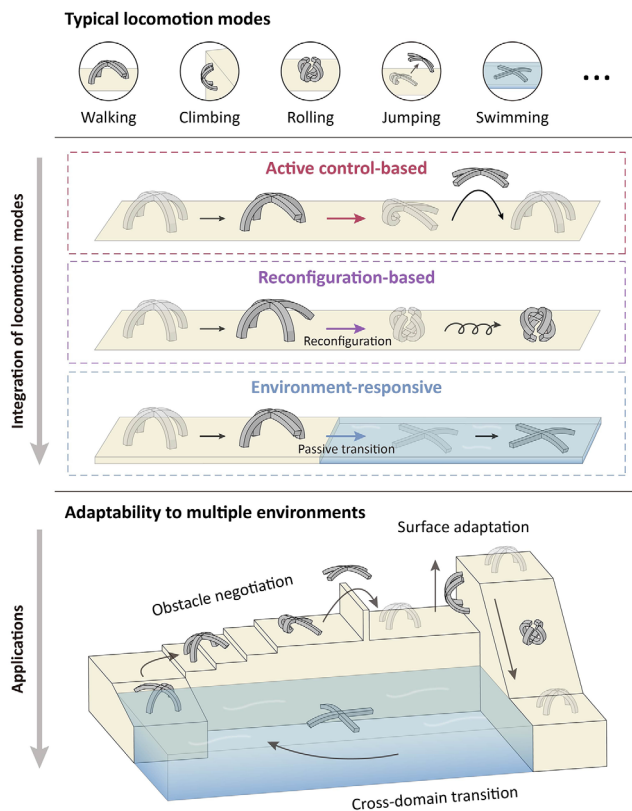


Figure 1. Multimodal locomotion of soft robots for multi-environment applications. Soft robots that integrate multiple locomotion modes hold great promise for multi-environment applications by transitioning their locomotion modes in response to environmental changes.

speed, energy efficiency, payload-to-weight ratio, and application environment.

2.1. Crawling

Crawling, the most versatile and widely implemented locomotion mode in soft robotics, relies on continuous body-substrate interactions and axial deformations for propulsion. Unlike leg-dependent gaits, crawling exploits the robot's inherent compliance to achieve motion via friction modulation, adhesion control, or wave propagation, making it suited for unstructured terrains and confined environments. This mode is broadly categorized into three bio-inspired subtypes based on deformation kinematics: inchworm-like (two-anchor), earthworm-like (peristaltic), and snake-like (serpentine).

Inchworm-like crawling, inspired by caterpillars, employs a cyclic two-anchor mechanism driven by sequential axial deformation. This mechanism critically relies on anisotropic friction or adhesion, where the forward friction coefficient is lower than backward, enabling directional propulsion during body deformation. Early robotics implementations emulated elongation/shortening and anisotropic friction to achieve crawling motion, exemplified by silicone-bodied crawlers using shape memory alloys (SMAs),^[18] pneumatic actuators^[19] that achieved linear

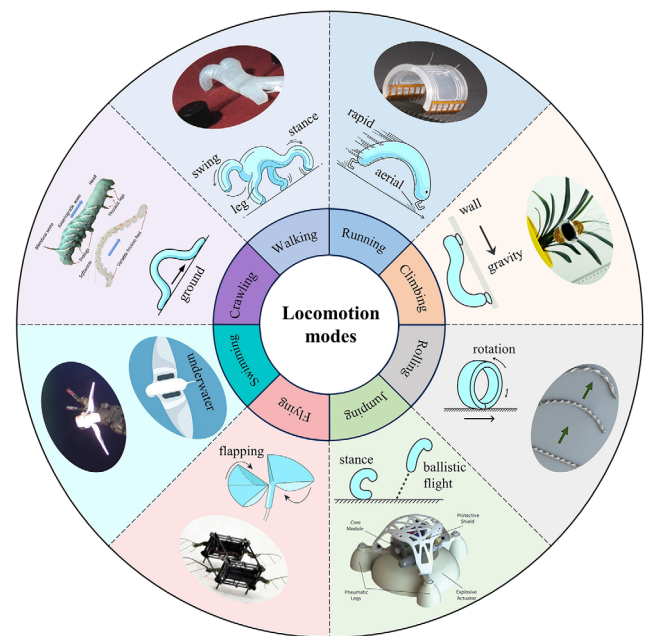


Figure 2. Overview of typical locomotion modes for soft robotics. Crawling: reproduced with permission.^[8] Copyright 2016, IOP Publishing. Walking: reproduced with permission.^[5] Copyright 2011, National Academy of Sciences. Running: reproduced under terms of the CC-BY license.^[40] Copyright 2022, The Authors, published by Springer Nature. Climbing: reproduced with permission.^[41] Copyright 2018, AAAS. Rolling: reproduced with permission.^[49] Copyright 2022, National Academy of Sciences. Jumping: reproduced with permission.^[53] Copyright 2015, AAAS. Flying: reproduced with permission.^[62] Copyright 2019, Springer Nature. Swimming: reproduced with permission.^[72] Copyright 2021, Springer Nature.

extension and contraction. Beyond pure linear deformation, elongation/shortening can also be functionally achieved by arching and flattening the central body, while anisotropic friction at the distal segments enables directional propulsion. Umedachi et al. developed a caterpillar-inspired soft robot with embedded SMA coils through sequential bending deformations and angle-dependent friction switching.^[8] Similarly, Zhu et al. created a light-driven soft robot that can crawl on land via asymmetric body bending and photothermally induced friction modulation.^[20]

Earthworm-like crawling draws inspiration from annelids, utilizing radially symmetric contraction waves that propagate axially along the body. This mode relies on muscular hydrostat mechanics: circumferential expansion coupled with longitudinal contraction in one segment generates localized anchoring, while adjacent segments undergo circumferential contraction and longitudinal extension to produce forward thrust. Crucially, directional propulsion stems solely from wave coordination, without inherent anisotropic friction. This principle is exemplified by Meshworm,^[21] a soft robot that employs antagonistic NiTi coils actuators within a braided mesh-tube structure to generate peristaltic waves for crawling. Recent advancements in earthworm-inspired robotics, such as a pneumatic soft robot enhanced by wire-winding transmission, demonstrate improved locomotion efficiency through coordinated segment deformation and overlapped peristaltic wave control, achieving speeds surpassing previous similar designs.^[22]

Table 1. Summary of typical locomotion modes for soft robotics.

Locomotion mode	Subtype	Actuation	Speed [BL s ⁻¹]	Energy efficiency	Payload-to-weight ratio	Application environment	Description	Ref.
Crawling	Inchworm-like crawling	Pneumatic	0.06	Low	N/A	Terrestrial	Utilize a two-anchor mechanism with anisotropic friction	[19]
		SMA	0.56	Low	N/A	Terrestrial, in-pipe		[8]
	Earthworm-like crawling	Pneumatic	0.036	Low	N/A	Terrestrial, in-pipe	Propagate radial or longitudinal waves via muscular hydrostat mechanics	[22]
		SMA	0.1	Low	N/A	Terrestrial		Generate lateral body waves propagating axially, requiring anisotropic friction
Walking	–	Pneumatic	0.008	Medium	0.44	Terrestrial	Coordinate discrete leg-ground interactions through cyclic stance-swing phases	[27]
		Electro-pneumatic	0.91	Medium	1.43	Terrestrial		[30]
		SMA	0.05	Medium	2.61	Terrestrial		[31]
Running	–	DEA	20.6	High	17	Terrestrial	Achieve dynamic stability via rapid cyclic deformation, featuring brief aerial phases	[35]
		DEA+SMA	2.02	High	2.9	Terrestrial		[36]
		Magnetic	70	High	N/A	Terrestrial		[40]
Climbing	–	DEA	0.75	Low	N/A	Wall	Maintain adhesion to vertical/inverted surfaces while resisting gravitational detachment	[41]
		DEA	0.71	Low	4	Wall, inverted plane		[42]
Rolling	–	SMA	2	High	N/A	Terrestrial	Enable continuous locomotion via wheel-ground contact with rotational motion	[46]
		DEA	4.59	High	N/A	Terrestrial		[48]
		Pneumatic	0.95	High	0.51	Terrestrial		[50]
Jumping	–	Combustion driven	5.8	Low	22	Terrestrial	Achieve ballistic flight via rapid energy release, generating impulsive momentum during stance phase	[54]
		Electric	6.01	Low	1.82	Terrestrial, obstacle		[55]
Flying	Flapping wing	DEA	N/A	Medium	N/A	Aerial	Produce lift and drag forces via reciprocating wing motions at high frequency.	[62]
		DEA	N/A	Medium	2.5	Aerial		[63]
	Morphing wing	Motor driven	N/A	Medium	N/A	Aerial	Dynamically reconfigure wing geometry during flight	[64]
Swimming	Undulation	DEA	0.009	Low	N/A	Aquatic	Generate thrust via whole-body traveling waves	[67]
	Rotational propulsion	Magnetic	0.23	Low	N/A	Aquatic	Induce propulsion through externally torqued spinning at low Reynolds numbers	[69]
	Lift-induced propulsion	DEA	0.69	High	N/A	Aquatic	Use oscillating fins to generate lift forces	[71]
	Drag-induced propulsion	Magnetic	N/A	Medium	N/A	Aquatic	Use paddle-like appendages to row through water	[74]
	Jet propulsion	Light driven	0.067	Medium	N/A	Aquatic	Exploit fluid momentum via cyclic ingestion and expulsion	[75]

Notes: The qualitative assessments for energy efficiency (low, medium, and high) are based on a relative comparison among different locomotion modes within the same actuation method. They do not represent an absolute efficiency comparison across different actuation methods. BL s⁻¹, body length per second. N/A, not available.

Snake-like crawling relies on propagating lateral body waves to generate directional thrust through controlled frictional asymmetry. Unlike peristalsis, it necessitates anisotropic friction: forward transverse friction must exceed backward axial friction to convert lateral undulations into net propulsion. This mechanism is demonstrated in a soft robotic snake composed of fluidic elastomeric

actuators,^[6] which achieves autonomous undulatory locomotion through traveling sinusoidal curvature waves and passive wheels that enforce frictional anisotropy. Callie et al. also developed a modular soft snake robot capable of implementing gait cycles to mimic lateral undulation.^[23] Friction modulation strategies in snake-inspired crawlers have been further explored through

kirigami skins for dynamic texture-based friction modulation during elongation^[24,25] and anisotropic surfaces patterned with directional friction materials.^[26]

2.2. Walking

Walking in soft robotics leverages discrete, cyclic leg-substrate interactions to achieve propulsion, contrasting with continuous body-substrate contact in crawling. This mode relies on two core mechanisms: 1) sequential stance-swing phases of deformable legs generating discrete ground reaction forces and 2) spatiotemporal synchronization of leg motions ensuring continuous forward thrust. The evolution of soft robotics walking locomotion stems from material innovations enabling compliant legged systems. Shepherd et al. pioneered this domain with a pneumatically actuated quadrupedal soft robot capable of legged gait generation through asymmetric chambers to induce bending.^[5] Subsequent work achieved autonomy with integrated onboard compressors, valves, and control system, creating fully untethered platforms.^[27] Van Laake et al. developed fluidic relaxation oscillators for reprogrammable leg actuation sequences, enabling electronic-free gait control in quadrupedal walkers.^[28] Pneumatic innovations extended to precharged actuators employing mechanical energy storage,^[29] while recent electro-pneumatic designs combine ultralight structures with high-force output for dynamic walking performance.^[30] Miniaturization efforts achieved insect-scale autonomy, as seen in Yang et al.'s 88-mg crawler utilizing catalytic artificial muscles for discrete leg actuation cycles.^[31] Light-driven implementations emerged through liquid crystal elastomer (LCE)-based microrobots^[32] and polarization-modulated photothermal walkers,^[33] both demonstrating spatiotemporal synchronization of deformable legs. These developments collectively validate two core mechanisms, which are realized across diverse materials from elastomeric polymers to stimuli-responsive composites and expand the operational envelope in terms of scale, autonomy, and locomotor efficiency.

2.3. Running

Soft robotic running fundamentally differs from walking by leveraging dynamic stability through elastic energy cycling and transient ground interactions. Rapid cyclic deformation of compliant actuators stores kinetic energy during compression and explosively releases it for propulsion, mimicking biological tendon-muscle systems. This process generates brief aerial phases that reduce ground friction while conserving momentum. Dielectric elastomer actuators (DEAs) excel in this domain. Zhao et al. demonstrated a DEA-driven hopping-running robot with exceptional adaptability to rough terrain, leveraging DEAs' rapid energy cycling for dynamic locomotion.^[34] Feng et al. enhanced DEA performance for high-speed running via optimized viscoelastic hysteresis and energy recirculation.^[35] Yang et al. further combined DEAs with SMA springs, achieving a running speed of 91 mm s⁻¹ in a compact 3.5 g robot.^[36] Dynamic control is achieved via spatiotemporal stiffness modulation, as demonstrated by spiral-shaped piezoelectric PVDF-copper composites that synchronize high-frequency actuation with mechanical resonance modes for ultrafast motion.^[37] Similarly, Park et al.'s soft

legged robot uses pre-curved piezoelectric legs and asymmetric actuation for animal-like running gaits.^[38] Insect-scale platforms, such as ultrarobust designs capable of withstanding extreme loads, maintain fast locomotion stability through asymmetric foot-ground interaction modulation and structural resilience.^[39] Mao et al. also introduced a small-scale soft electromagnetic robot using liquid metal coils, achieving ultrafast, multifunctional locomotion under resonant actuation in static magnetic fields.^[40] These advances significantly advance the development of high-speed, agile soft robotics running through elastic energy cycling and sophisticated dynamic control.

2.4. Climbing

Soft robotic climbing confronts the fundamental challenge of overcoming gravity during vertical or inverted surface traversal. While often employing similar gaits like crawling, climbing necessitates strong, directional adhesion sufficient to anchor against gravity, primarily generating normal forces perpendicular to the surface. Crucially, the robot's actuation must produce an upward force to lift itself, demanding synchronized adhesion-actuation cycles with precise timing for secure anchoring and efficient detachment. Energy expenditure is dominated by gaining potential energy, making climbing a distinct locomotion mode defined by its gravity-counteracting mechanics. This challenge was successfully addressed by a tethered soft climbing robot, which pioneered a mechanism integrating dielectric elastomer artificial muscles for body deformation and electroadhesive feet with spatiotemporal adhesion control.^[41] Hu et al. further designed a robot capable of inverted climbing by assembling the acrylic stick-constrained dielectric elastomer actuator with a flexible support frame.^[42] Subsequent innovations overcome tethering and environmental constraints through distinct strategies. For example, Lee et al. achieved electronics-free climbing using buckling-sheet ring oscillators, where anisotropy friction converts sheet buckling into directional thrust.^[43] Pang et al. enabled climbing on complex surfaces via voltage-controlled shape-morphing footpads and stiffness-tunable smart joints.^[44] Wu et al. introduced magnetically driven peeling-and-loading mechanics with mucus-penetrating microstructured adhesives, enabling stable climbing on wet biological tissues.^[45]

2.5. Rolling

Rolling in soft robotics exploits continuous rotational motion around a stable axis or instantaneous center of rotation. Cyclic deformation of compliant actuators generates unidirectional angular momentum, translating directly into directional displacement. This persistent wheel-ground contact minimizes sliding friction losses and leverages inherent structural compliance for passive terrain adaptation. Early breakthroughs emerged from bio-inspired ballistic rolling, utilizing rapid body morphing for impulsive propulsion as demonstrated in caterpillar-like robots.^[46] Subsequent advances harnessed stimuli-responsive materials: LCE-based origami robots achieved rolling through selective thermal actuation of embedded hinge patterns,^[47] while dielectric elastomer systems generated high-speed ballistic rolling through controlled anchoring and voltage.^[48] Recent

advances prioritize environmental adaptation through synergistic material-architectural innovations. Twisted LCE ribbons uniquely enable autonomous obstacle negotiation by triggering directional self-snapping instabilities during rolling.^[49] Other strategies include pneumatically driven systems reconfiguring ground contact via elastic buckling for terrain traversal,^[50] helical filaments modulating travel paths through thermal geometry tuning,^[51] and dual helices sustaining propulsion via humidity-activated alternating cycles.^[52] These innovations collectively validate engineered compliance for context-aware rolling functionality.

2.6. Jumping

Soft robotic jumping is governed by two distinct phases: a ground-contact stance phase for quasi-static energy storage in deformable structures and a subsequent ballistic flight phase triggered by crossing a critical instability threshold. During stance, soft actuators gradually store potential energy via controlled deformation, whose abrupt release generates impulsive momentum for ballistic propulsion. Trajectory control arises from asymmetric force distribution, while material compliance ensures impact resilience. This temporal decoupling of energy accumulation and explosive release enables obstacle clearance beyond continuous locomotion capabilities. Bartlett et al. manufactured a combustion-driven robot using multimaterial three-dimensional printing, establishing pressure-triggered phase transitions as a paradigm for untethered jumping.^[53] This approach was subsequently miniaturized by an insect-scale quadrupedal robot with high power densities.^[54] Recent advances have refined this paradigm through novel actuator designs and bioinspired strategies. Chen et al. developed a legless soft rapid continuous jumper, converting dielectric liquid redistribution into directional momentum while leveraging elastic frame rebound for vertical propulsion.^[55] A multidirectional jumper driven by a single biaxial electrohydraulic actuator was further introduced, whose asymmetric electrode patterning enabled four-directional jumps without auxiliary steering mechanisms.^[56] Besides, Wang et al. reported a bistable soft jumping robot manufactured by 4D printing of composites with continuous fibers, exploiting temperature-triggered snap-through for multimodal jumping.^[57] For fluidic environments, Koh et al. decoded the surface tension-dominated jumping of water striders, revealing that leg rotation maximizes momentum transfer by maintaining meniscus contact below the rupture threshold.^[58] Overall, these advances demonstrate how tailored structural design and stimuli-responsive actuation enable energy-efficient jumping with directional control across diverse environments.

2.7. Flying

Aerial locomotion is challenging due to the stringent thrust-to-weight ratio required for lift generation. Soft flying robots address this by leveraging adaptive morphology and compliant aerodynamics to achieve efficient aerial mobility. Unlike rigid-wing systems, they exploit material elasticity to dynamically reconfigure wing shape during flight, enabling enhanced

maneuverability, disturbance rejection, and energy efficiency through passive or active deformation. This bioinspired approach primarily adopts two strategies: flapping wing or morphing wing.

Flapping wing robots, mimicking birds and insects, generate lift and drag forces via reciprocating wing motions. While many existing systems are driven by rigid actuators (e.g., piezoelectric bimorphs, electromagnetic motors),^[59–61] recent progress in soft-actuated flapping-wing robots offers complementary advantages such as mechanical resilience, reduced complexity, and improved endurance. Notably, soft actuators have achieved sufficient power density to enable sustained flight. For instance, Chen et al. designed a microrobot powered by dielectric elastomer artificial muscles, achieving a power density of 600 W kg^{-1} while enabling collision-resilient and controlled flight.^[62] Ren et al. further developed a low-voltage, high-endurance, and power-dense DEA for a sub-gram soft aerial robot, achieving a high lift-to-weight ratio and long hovering flight. These soft-actuated systems demonstrate performance comparable to rigid-powered flapping wing robots in key metrics like power density and flight stability.^[63]

Morphing wing systems dynamically reconfigure wing geometry in flight to optimize aerodynamics. Unlike flapping wing, morphing wing is inspired by bird flight adaptations like forward-sweeping wings and fanned tails during slow maneuvers. Recent biohybrid designs replicate avian skeletal mechanics through feather-ligament coupling, enabling high-bandwidth roll control via underactuated wrist and finger motion.^[64] Beyond isolated wing morphing, integrated wing-tail systems leverage foldable artificial feathers to synergistically expand surface areas, enhancing lift generation and roll authority beyond rigid ailerons.^[65] Advancing structural adaptability, digitally assembled lattice wings deploy programmable stiffness gradients, combining rigid and flexible components to achieve span-wise twist deformation for stall resistance at ultralight densities.^[66]

2.8. Swimming

Aquatic locomotion presents hydrodynamics challenges distinct from aerial environments, demanding specialized thrust generation strategies. Soft swimming robots address these by leveraging body compliance and fluid-structure interactions to achieve efficient propulsion through five primary bioinspired mechanisms: undulation, rotational propulsion, lift-induced propulsion, drag-induced propulsion, and jet propulsion.

Undulation, mimicking slender-bodied fish (e.g., eels, rays), employs whole-body traveling waves to generate thrust. This mechanism propagates axial or lateral body bends rearward, creating momentum exchange with surrounding fluid. For example, a translucent eel-inspired robot leveraged frameless fluid electrode DEAs, where sequential activation creates axial undulation waves, achieving 52% Froude efficiency while maintaining optical stealth.^[67] Advancing to wave programming, Shahsavan et al. demonstrated programmable photothermal undulation in liquid crystal gels, where directional light triggers asymmetric curvature waves to control propulsion direction and achieve multimodal swimming.^[68]

In microswimmer propulsion, the rotational mechanism exploits externally torqued spinning of compliant structures

(e.g., helical filaments) to generate thrust through nonreciprocal deformation at low Reynolds numbers. This mechanism, inspired by bacterial flagella, relies on fluid-structure interactions that dynamically reshape morphology. Stiffness-tunable magnetic hydrogels harness this principle to achieve helical coiling of soft tails, enabling adaptive screw propulsion across fluid viscosities.^[69] Critically, Xu et al. revealed that pitch collapse induces dynamic stops at a morphological step-out frequency, while further increasing the rotation frequency of the magnetic field inverts tail chirality to generate reverse thrust.^[70]

In contrast, larger-sized organisms (e.g., manta, tuna) typically use fins or flukes for lift-induced propulsion, harnessing hydrofoil principles akin to aerial flight. Oscillating fins produce pressure differentials, generating sufficient lift forces under inertia-dominated conditions. Similarly, a manta ray-inspired soft robotic fish using DEAs strategically leveraged surrounding water as an electrode, enabling efficient flapping-fin swimming without rigid insulation components.^[71] Notably, Li et al. achieved breakthrough deep-sea lift propulsion through flapping pectoral fins, validated at 10 900 m depth in the Mariana Trench.^[72] The robot's performance demonstrated functional lift generation under extreme pressure.

Unlike lift-induced swimming that gains thrust from hydrodynamic lift, drag-induced propulsion exploits directional asymmetry in fluid resistance to generate net thrust. This mechanism mimics semiaquatic organisms (e.g., beetles) that use paddle-like appendages to row through water. Inspired by such organisms, Jia et al. engineered a surface-swimming robot with propulsors of graded flexural rigidity, which unfolds during power strokes for maximal propulsion area and compliantly folds in recovery strokes for low resistance, achieving enhanced energy efficiency.^[73] Similarly, a jellyfish-like millirobot replicated asymmetric lappet kinematics that amplify thrust during contraction and reduce drag in recovery, enabling efficient fluid control in moderate Reynolds regimes.^[74]

In addition, some organisms (e.g., squid) achieve pulsatile swimming by jet propulsion, which exploits fluid momentum via cyclic ingestion and expulsion. This mechanism inspires the design of soft pulsatile swimming robots. For example, Godaba et al. designed a DEA where voltage-triggered membrane expansion generates pulsatile thrust and buoyancy modulation for vertical propulsion in a jellyfish-like robot.^[9] Periodic liquid or gas generation is an alternative approach, as demonstrated by a light-powered soft oscillator using photothermal steam bubbles to drive pulsed swimming, enabling adaptive locomotion through tunable fluid expulsion frequencies.^[75]

3. Mechanisms of Multimodal Locomotion

Although soft robots have demonstrated impressive locomotion capabilities, most of them merely exhibit a single type of locomotion mode. The prevailing trend is to integrate multiple locomotion modes within a single robotic system to enable adaptability across diverse scenarios. Besides, it is equally important to achieve transitions between distinct locomotion modes. In this section, we delve into the underlying mechanisms of multimodal locomotion, classifying them into three primary categories:

active control-based, reconfiguration-based, and environment-responsive strategies.

3.1. Active Control-Based Strategy

A significant number of soft robots employ active control-based strategies to achieve multimodal locomotion. One straightforward approach involves integrating multiple actuators into the robot's body to provide sufficient degrees of freedom (DoF). An early example is a five-module soft robot, each module incorporating three vacuum-powered soft pneumatic actuators.^[76] Binary activation signals were applied to each actuator, and the fifteen actuators were coordinated to achieve two distinct gaits: crawling and rolling (Figure 3a). Similarly, a *Drosophila* larvae-inspired soft robot was developed with three serially connected modules, each containing four SMA coils.^[77] The additional DoF in each module allowed the robot to execute more complex locomotion modes such as turning and twisting. Despite these advances, physical space constraints and power requirements often limit the number and variety of actuators that can be incorporated into robots, ultimately restricting their locomotion capabilities. To overcome this challenge, a hierarchical actuation design for multi-appendage soft robots was proposed.^[78] In this design, a single high-power motor actuated all appendages for locomotion, while smaller low-power motors augmented the shape of each appendage. This arrangement enables the robot to perform a variety of multimodal locomotion behaviors, including swimming, turning, grasping, and crawling (Figure 3b).

Many studies employ untethered actuation via external fields to achieve programmable multimodal locomotion, significantly reducing the requirement for embedded discrete actuators by leveraging spatially programmed materials.^[79,80] A representative example is a magneto-elastic soft robot embedded with neodymium-iron-boron (NdFeB) microparticles and programmed with a single-wavelength harmonic magnetization profile along its body.^[81] By modulating the magnitude, phase, and frequency of the applied magnetic field, the robot achieved various locomotion modes, including crawling, rolling, jumping, and swimming (Figure 3c). Magnetic soft robots exhibiting such multimodal locomotion have shown considerable promise in biomedical applications, such as targeted drug delivery and release, particularly when combined with advanced imaging techniques, including ultrasound, X-rays, and magnetic resonance imaging.^[82] Another example is a *Pleurotya* caterpillar-inspired light-driven soft robot with multiple postures.^[83] The segmental robot was fabricated by advanced multi-material 4D printing with programmable mesogen alignment. Spatially resolved near-infrared irradiation induced localized photothermal effects in targeted LCE segments, enabling on-demand curvature modulation. This actuation strategy supported adaptive locomotion behaviors, including bidirectional crawling, rolling, and self-righting (Figure 3d).

Recently, several studies have demonstrated that frequency modulation can induce multimodal locomotion even in robots with limited DoFs by leveraging their dynamic behavior. One such example is a dexterous electrical-driven soft robot featuring a chiral-lattice foot.^[84] By modulating the voltage frequency, the robot could control whether the chiral-lattice foot remained in contact with the substrate or lifted off, thereby enabling forward or

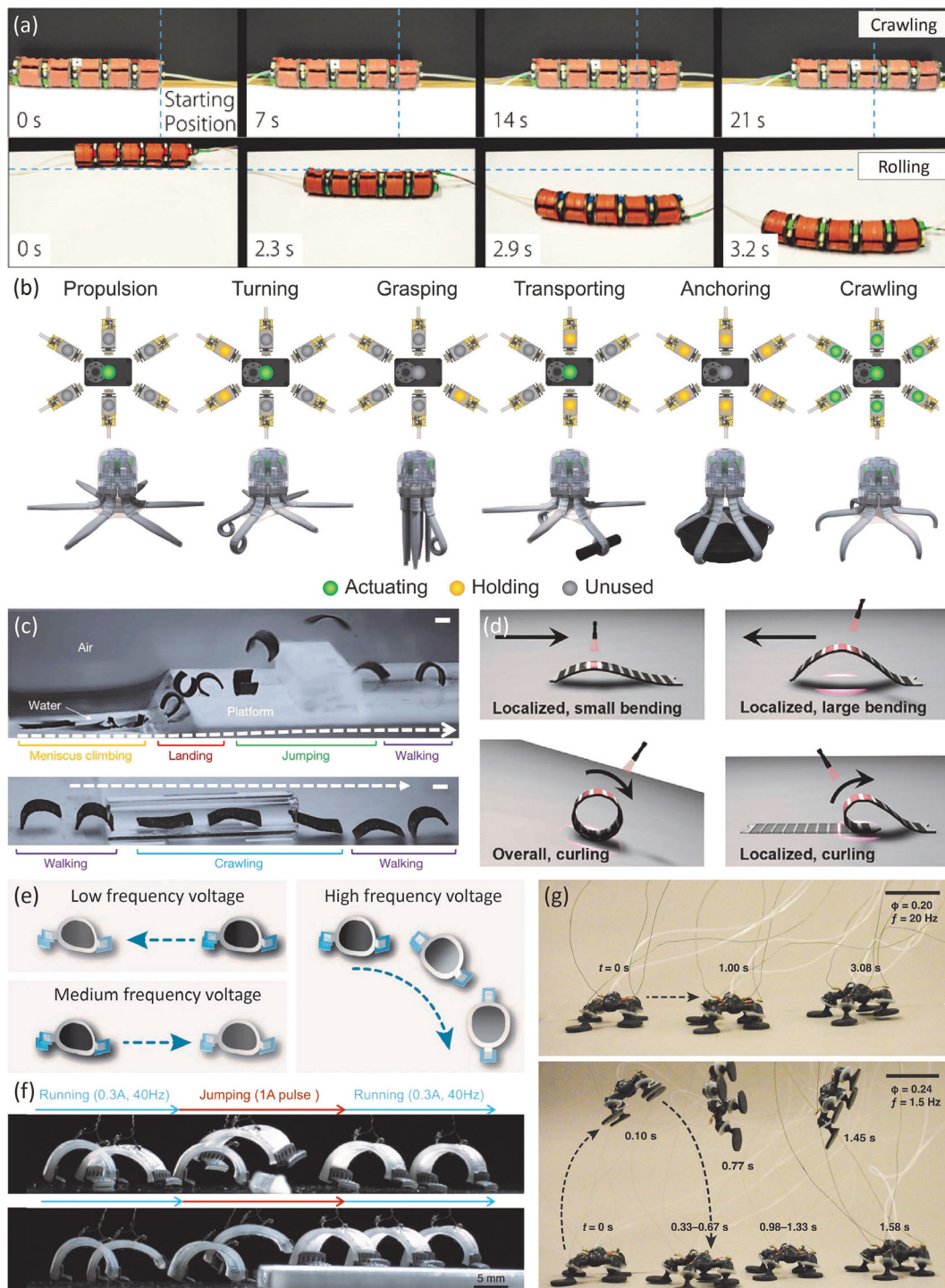


Figure 3. Multimodal locomotion of soft robots via active control-based strategies. a) A vacuum-powered multi-module soft robot capable of crawling and rolling via gait control. Reproduced with permission.^[76] Copyright 2017, AAAS. b) A hierarchical actuation design for multi-appendage soft robots enabling efficient multimodal locomotion. Reproduced with permission.^[78] Copyright 2024, Mary Ann Liebert, Inc. c) A magneto-elastic millimeter-scale soft robot capable of multimodal locomotion by modulating the applied magnetic field. Reproduced with permission.^[81] Copyright 2018, Springer Nature. d) A *Pleurotaya* caterpillar-inspired segmental robot for adaptive locomotion through spatially resolved near-infrared irradiation. Reproduced with permission.^[83] Copyright 2025, Wiley. e) A small-scale, dexterous soft robot capable of reaching arbitrary points in a plane under a single voltage input. Reproduced under terms of the CC-BY license.^[84] Copyright 2023, The Authors, published by Springer Nature. f) A small-scale soft robot capable of both running and jumping using a single electromagnetic actuator. Reproduced under terms of the CC-BY license.^[40] Copyright 2022, The Authors, published by Springer Nature. g) An insect-scale, combustion-driven quadrupedal robot exhibiting crawling at a high actuation frequency and hopping at lower frequencies. Reproduced with permission.^[54] Copyright 2023, AAAS.

backward locomotion. As the frequency approached its resonance frequency, the robot moved circularly due to the synergistic effect of the dynamic resonant and chiral twisting (Figure 3e). Another example is a spiral-shaped piezoelectric soft robot capable of bidirectional locomotion by utilizing different vibration modes at higher-order resonance frequencies.^[37] The robot exhibited forward locomotion at 76 body lengths per second under first-order resonance and backward locomotion at 11.26 body lengths per second under third-order resonance. Furthermore, frequency modulation can also induce distinct locomotion modes. A small-scale soft robot was reported capable of both running and jumping using a single electromagnetic actuator.^[40] Embedded liquid metal coils generated Lorentz forces when subjected to alternating current within a static magnetic field, resulting in frequency-dependent vibrations. The robot achieved high-speed running near its resonant frequency and was capable of jumping over obstacles by storing and releasing energy through pulsed current inputs (Figure 3f). Similarly, an insect-scale, combustion-driven quadrupedal robot demonstrated both crawling and hopping by modifying the fuel equivalence ratio and the sparking frequency (Figure 3g).^[54] In general, these innovative studies highlight the strategic use of frequency modulation, either by tuning resonance or exploiting dynamic interactions with the environment, to achieve multimodal locomotion.

3.2. Reconfiguration-Based Strategy

Reconfiguration capability enables soft robots to adapt their morphology and functionality, facilitating the realization of multimodal locomotion. An early example is a pneumatic soft robot utilizing shape change to traverse both flat and inclined surfaces.^[85] The robot featured an internal bladder for shape modification and a set of external bladders for propulsion. On flat terrain, it achieved rolling locomotion by sequentially inflating the trailing-edge bladder (Figure 4a). When encountering inclines that hindered rolling, the robot deflated its inner bladder to transition into a flattened configuration. By simultaneously inflating the four upward-facing bladders, the robot employed an inchworm-like gait to climb inclines. In addition to fully soft-bodied robots, soft materials are increasingly employed as morphing elements in reconfigurable robots that incorporate rigid components. One study demonstrated that combining compliant structures with morphological reconfiguration enabled autonomous multimodal locomotion across complex terrains with minimal sensing.^[86] Lens-like structures were leveraged to tune torsional stiffness, allowing the robot to transform from a flat rover for driving to a spherical shape for rolling (Figure 4b). By actively reconfiguring its morphology, such as adjusting its aspect ratio for optimized speed and drift, or redistributing its payload for self-instigate rolling, the robot improved its locomotion performance in diverse and rough environments.

A typical approach to achieving such reconfiguration involves variable-stiffness structures. Inspired by terrestrial and aquatic turtles, a robotic turtle was developed that combined rigid components with soft materials to enable limb shape changes and gait switching for amphibious locomotion.^[87] The morphing limb consisted of an antagonistic pneumatic actuator pair with strain-limiting layers adhered to thermoset polymers. Heating

the thermosets through embedded heaters and inflating the pneumatic actuators increased the limb's cross-sectional area and storage modulus, enabling transitions between a cylindrical geometry for walking and a flat flipper geometry for swimming (Figure 4c). Another study introduced continuously morphable actuators that combined programmable deformation via LCEs with stiffness locking through shape memory polymers.^[88] A lightweight terrestrial-aerial microrobot employing these actuators was demonstrated. One pair of actuators switched the function of propellers between rotor wings (aerial mode) and wheels (terrestrial mode), while another pair assisted the control of propeller gestures by adjusting the undercarriages (Figure 4d). In summary, these designs exploit the temperature-induced variable-stiffness properties of soft materials to enable reconfiguration. Their high stiffness at low temperatures offers excellent load-bearing capacity without continuous actuation, making them ideal for hybrid soft-rigid systems.

Another notable approach leverages bistable structures, which provide both shape-locking capability in stable states and active-morphing capability through snap-through transitions. One example involves a soft actuator incorporating bistable chiral metamaterials and tube-sealed SMA for a morphable multimodal robot designed for deep-sea exploration.^[89] The chiral unit was precompressed from a cross-shaped soft precursor to exhibit left-handed and right-handed stable states. Upon activation of the SMA springs, the front chiral unit was reconfigured, allowing the robot to transition from swimming to crawling mode within 0.75 s after landing (Figure 4e). While reconfigurable designs enhance locomotion versatility, they typically require dedicated actuators for shape morphing, increasing system complexity. To address this, a snap inflatable modular metastructure was developed to enable multiple reversible configurations using only a single pressure input.^[90] The metastructure consisted of interconnected snap units, each comprising a pneumatic cell attached to a spherical bistable elastomeric shell. A soft robot constructed by aligning three extension-snap modules, each with snap units attached to both ends of a pneumatic bellow, could transition between flat and cylindrical shapes, and elongating or recover in both configurations. This allowed the robot to achieve planar crawling and cable climbing using only a single pressure input (Figure 4f).

3.3. Environment-Responsive Strategy

Recently, researchers have explored several designs that can passively transition between locomotion modes in response to environmental changes. One example is an origami robot capable of self-adaptive locomotion on unstructured terrain.^[91] A magnetic plate was affixed to one end of the Kresling origami. On flat ground, the robot demonstrated either rolling or flipping modes, achieved by rotating the magnetic field in a plane perpendicular or parallel to the robot's longitudinal axis, respectively. When encountering obstacles, the robot automatically switched between rolling and flipping modes to navigate the terrains while maintaining its moving direction, without requiring any modification to the magnetic control input (Figure 5a). Another example is an LCE robot capable of self-sustained multimodal locomotion by tuning the substrate adhesion.^[92] The robot

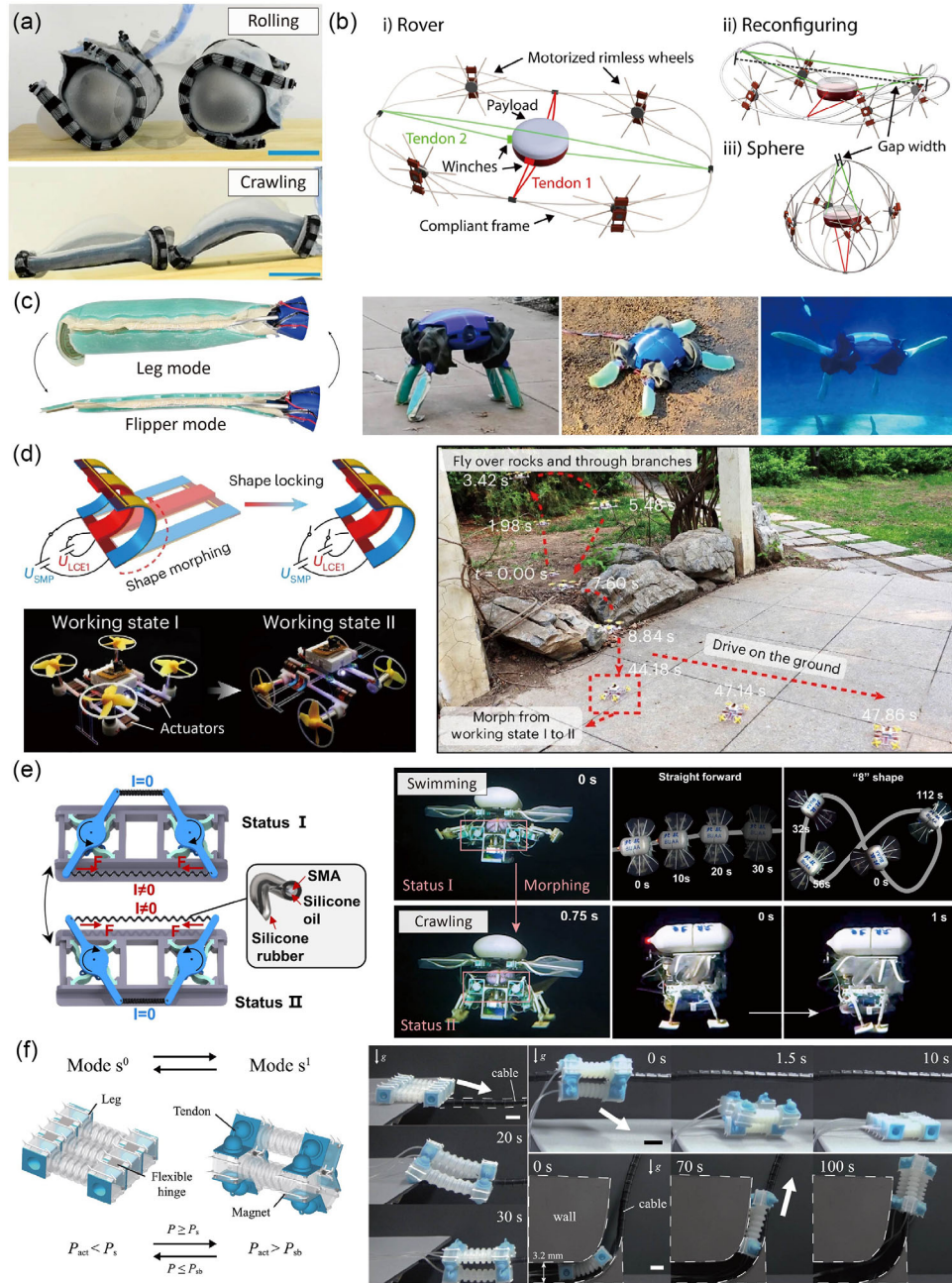


Figure 4. Multimodal locomotion of soft robots via reconfiguration-based strategies. a) A pneumatic soft robot utilizing shape change to traverse both flat and inclined surfaces. Reproduced with permission.^[85] Copyright 2020, Springer Nature. b) Combining compliant structures with morphological reconfiguration enabling autonomous multimodal locomotion across complex terrains with minimal sensing. Reproduced with permission.^[86] Copyright 2025, AAAS. c) An Amphibious Robotic Turtle combining rigid components and soft materials to enable augmented limb shape changes and gait switching for amphibious locomotion. Reproduced with permission.^[87] Copyright 2022, Springer Nature. d) A lightweight terrestrial-aerial microrobot based on small-scale continuously morphable actuators that combine programmable deformation and stiffness locking. Reproduced with permission.^[88] Copyright 2025, Springer Nature. e) A morphable multimodal robot for deep-sea exploration based on soft actuators incorporating bistable chiral metamaterials and tube-sealed SMA. Reproduced with permission.^[89] Copyright 2025, AAAS. f) A soft robot consisting of snap inflatable modular metastructures capable of multimodal locomotion using only a single pressure input. Reproduced with permission.^[90] Copyright 2025, Elsevier.

was mechanically trained to undergo thermally driven, continuous shape shifting for autonomous locomotion. On a hotplate, asymmetric heating caused the robot to arch upward. Driven by inertia, the robot flipped twice and returned to its original

shape, resulting in continuous rolling. When placed on a high-adhesion surface (coated with viscous silicone oil), the robot stored more energy during arching, which triggered a jumping motion upon sudden release (Figure 5b).

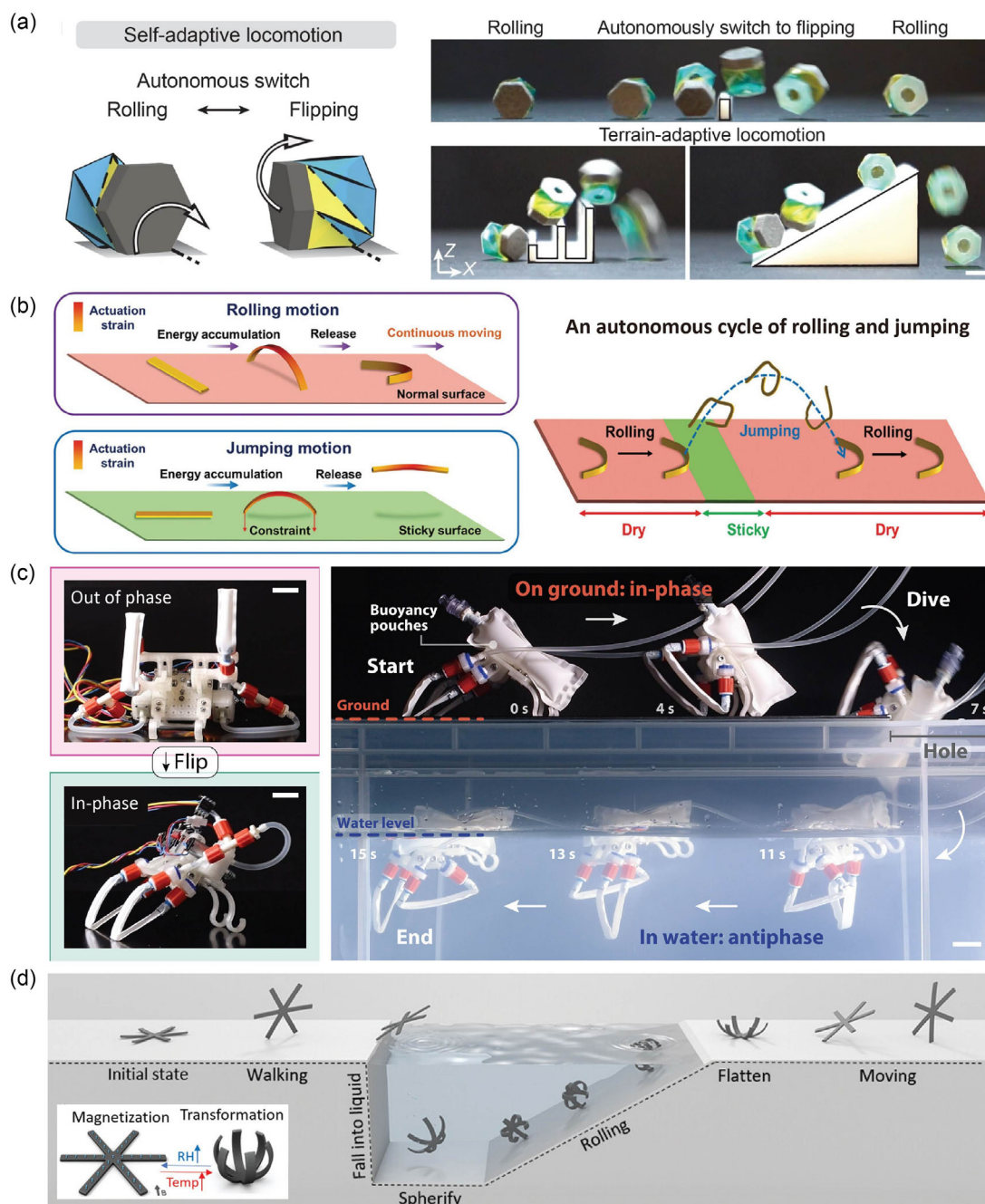


Figure 5. Multimodal locomotion of soft robots via environment-responsive strategies. a) An amphibious origami millirobot capable of self-adaptive locomotion on unstructured terrain. Reproduced under terms of the CC-BY license.^[91] Copyright 2022, The Authors, published by Springer Nature. b) An LCE robot capable of self-sustained multimodal locomotion, where the specific locomotion mode is controlled via substrate adhesion. Reproduced under terms of the CC-BY license.^[92] Copyright 2024, The Authors, published by Wiley. c) A soft-limbed robot with embedded fluidic circuits utilizing implicit environmental coupling for fast and autonomous locomotion. Reproduced with permission.^[93] Copyright 2025, AAAS. d) A multi-stimuli-responsive soft robot capable of reacting to six environmental stimuli: humidity, heat, light, radio frequency heating, low-frequency magnetic fields, and chemical solvents. Reproduced under terms of the CC-BY license.^[94] Copyright 2023, The Authors, published by Wiley.

Transitioning between solid and fluid environments can also reshape a robot's dynamic behavior. A soft-limbed robot with embedded fluidic circuits demonstrated fast and autonomous locomotion through implicit environmental coupling.^[93] The

untethered robot comprised two pouch tubes as soft limbs. An individual soft limb exhibited periodic and asymmetric motions by harnessing a self-oscillating behavior of thin soft tubes. When the robot was placed upside down, the two limbs were

out of phase under actuation at different natural frequencies. However, when the robot was placed upright so that the limbs contacted the ground, the two limbs synchronized their motion and actuated in-phase, resulting in hopping locomotion. Notably, upon immersion in water, the robot autonomously transitioned from its in-phase hopping gait to an antiphase swimming gait without any morphological changes or control input (Figure 5c). These transitions illustrated how external cues could affect the coupling between the body dynamics and the environment.

Environment-responsive shape morphing also offers a promising route to adaptive multimodal locomotion. A magnetic soft robot was developed featuring a sandwich structure formed by bonding a superhydrophilic hydrogel and a superhydrophobic elastomer via a laser-induced graphene layer.^[94] This structure enabled shape morphing in response to six environmental stimuli: humidity, heat, light, radio frequency heating, low-frequency magnetic fields, and chemical solvents. Under ambient conditions (room temperature and 90% relative humidity), the robot maintained a flat configuration and demonstrated walking behavior. Upon falling into ethanol, which absorbed moisture from the robot, it spontaneously morphed into a spherical configuration, enabling rolling locomotion on a sloped surface (Figure 5d). After exiting the liquid, the adsorbed ethanol rapidly evaporated, and the robot reabsorbed ambient moisture, returning to its original flat shape. Compared with the examples presented in Section 3.2 that reconfigure actively, this environment-responsive shape morphing achieves passive reconfiguration without the need for dedicated reconfigurable actuators, thereby reducing structural complexity.

3.4. Comparison among Three Strategies

The three representative strategies for achieving multimodal locomotion exhibit distinct characteristics and trade-offs (Table 2). Among them, the active control-based strategy is the most widely adopted and straightforward, realizing multimodal locomotion through multi-degree-of-freedom actuation. The availability of diverse controllable variables, such as amplitude, frequency, phase, and spatial distribution, offers high programmability and flexibility, but this advantage often comes at the expense of increased structural complexity and control complexity. For more substantial changes in locomotion modes (e.g., transitioning from walking to flying), the reconfiguration-based strategy often becomes necessary, enabling robots to adapt their morphology for efficiently generating specialized locomotion modes. Advanced designs can even incorporate both shape-locking and active-morphing capabilities

with relatively low energy consumption, making them well suited for hybrid soft-rigid systems. Nevertheless, the process of reconfiguration generally requires additional actuators and operation time. The environment-responsive strategy offers a more autonomous and adaptive alternative by allowing robots to passively transition between locomotion modes in response to environmental changes, particularly suitable for cross-domain transition. This approach significantly reduces both structural and control complexity, embodying the concept of physical intelligence. Its main challenge lies in designing structures that reliably achieve desired deformations under environmental stimuli. Notably, the boundaries among these strategies are often blurred, and emerging designs increasingly integrate elements from multiple strategies to achieve enhanced adaptability and efficiency.^[94]

4. Adaptability to Multiple Environments via Multimodal Locomotion

While the prior section has outlined the technical foundations for achieving diverse locomotion modes, this section shifts focus to the active selection and deployment of appropriate modalities in response to dynamic environmental demands. The robust adaptability of organisms in nature is manifested not only through the integration of multiple locomotion modes but also in their ability to transition seamlessly across diverse environments.^[16] Achieving comparable adaptability in robotics remains a long-standing challenge. The contact interface dynamics can vary significantly across environments, necessitating smooth and adaptive mode transition capabilities. Robust transition control is particularly critical, as hazardous transient states induced by environmental uncertainties may propagate into irreversible mechanical failures.^[95] In response to these challenges, we focus on three representative adaptation scenarios: 1) cross-domain transition, between terrestrial, aquatic, and aerial environments; 2) surface adaptation, including transitions from horizontal planes to vertical walls and inverted ceilings; and 3) obstacle negotiation, which requires alternative modes for overcoming high barriers, traversing narrow gaps, or ascending staircases.

4.1. Cross-Domain Transition

While most organisms in nature possess the ability to move through diverse mediums, bionic soft robots remain largely constrained to locomotion within a single medium. To enhance robotic environmental adaptability, researchers leverage multimodal locomotion mechanisms to enable autonomous

Table 2. Comparison among three multimodal locomotion strategies.

Strategy	Principle	Advantages	Limitations	Representative examples
Active control-based strategy	Multi-degree-of-freedom actuation	High programmability and flexibility	Increased structural and control complexity	[37,40,54,76–78,81,83,84]
Reconfiguration-based strategy	Functional change via structural reconfiguration	Efficient generation of specialized locomotion modes	Require additional actuators and operation time	[85–90]
Environment-responsive strategy	Passive adaptation to environmental changes	Low structural and control complexity	Environment-dependent applicability	[91–94]

transitions between terrestrial, aquatic, and aerial environments. The aquatic-terrestrial transition stands as an exemplary paradigm for cross-domain locomotion. Due to its high engineering feasibility, diverse amphibious soft robotic prototypes have been developed. An ultrathin soft robot achieves seamless water-land transitions using electrostatic adhesion and biomimetic propulsion (Figure 6a).^[96] The robot combines DEA with tunable Poisson's ratio mechanisms to enable terrestrial crawling via electrostatic adhesive pads. For aquatic locomotion, detached rear pad serves as a tail fin to drive undulating swimming. This dual functionality of electrostatic adhesive pads as both terrestrial anchors and aquatic propulsion elements demonstrates

robust environmental adaptability. Such designs featuring structural multifunctionality of body components across varied environments represent a prevalent bionic paradigm. For instance, flippers of an arc-heating robot concurrently function as terrestrial planar limbs and aquatic propulsive fins,^[97] whereas robots composed of electrohydraulic actuators drive individual limbs to crawl on land while utilizing tripedal synchronization to achieve medusoid propulsion underwater.^[98]

Beyond inherent structural multifunctionality, functional modifications induced by structural reconfiguration provide an alternative way to achieve adaptive transitions. A shape-reconfigurable soft robot capable of multimodal locomotion

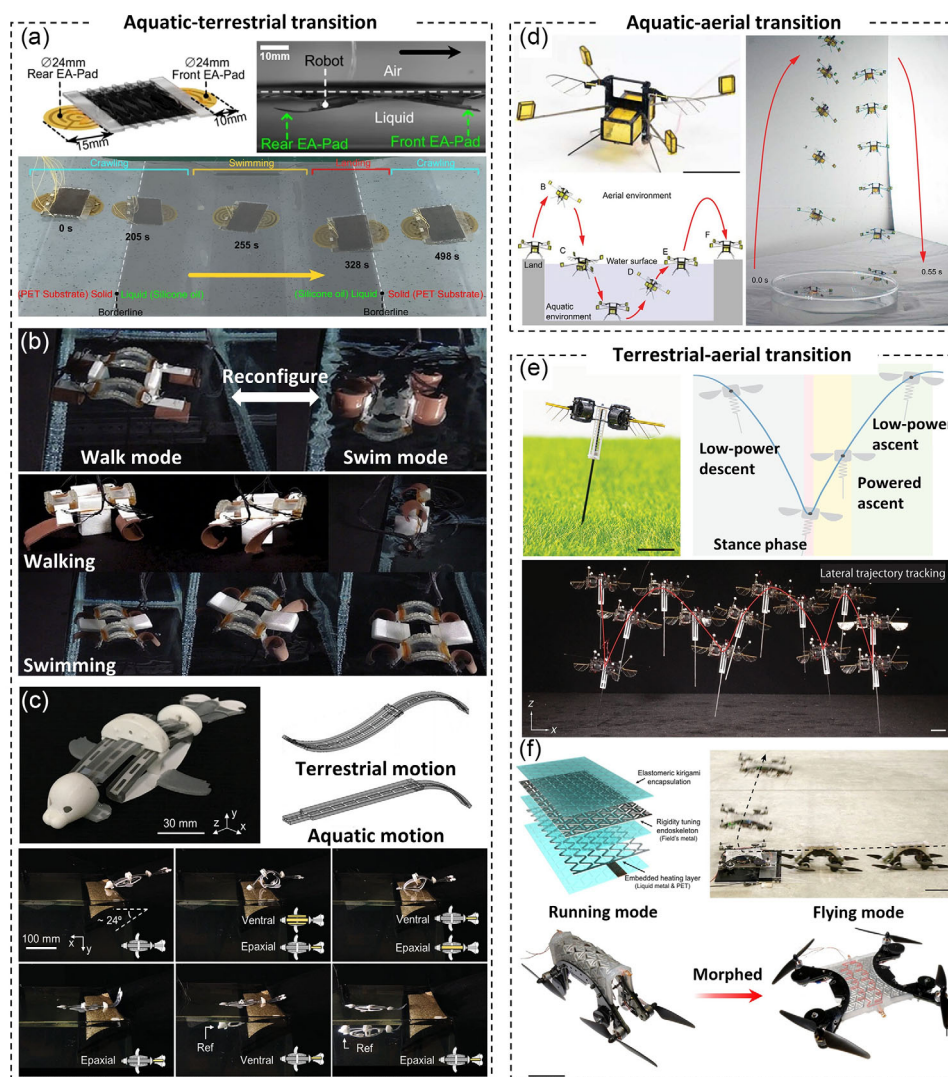


Figure 6. Adaptive multimodal locomotion transition across heterogeneous domains. a) An ultrathin soft robot utilizing electrostatic adhesion and biomimetic propulsion strategies to enable seamless water-land transitions. Reproduced under terms of the CC-BY license.^[96] Copyright 2024, The Authors, published by Springer Nature. b) An amphibious robot using bistable shape memory alloy actuators to shift from a quadruped crawler to a frog-like swimmer. Reproduced with permission.^[99] Copyright 2022, Wiley. c) A seal-inspired amphibious robot made of shape memory alloys that can crawl on land and swim in water. Reproduced with permission.^[100] Copyright 2022, Wiley. d) An insect-scale piezoelectric-driven microrobot capable of air-water multimodal locomotion. Reproduced with permission.^[101] Copyright 2017, AAAS. e) A hybrid microrobot driven by dielectric elastomer actuators integrating flapping wings and passive legs to enable terrestrial-aerial locomotion. Reproduced with permission.^[102] Copyright 2025, AAAS. f) A multifunctional shape-morphing metamaterial as an essential component of soft robotic drones that can run and fly. Reproduced with permission.^[103] Copyright 2022, AAAS.

was designed based on bistable soft actuators (Figure 6b).^[99] These actuators are composed of a prestretched membrane sandwiched between 3D printed frames with embedded antagonistic SMA coils. Due to the bistable structure, the robot can reconfigure from a quadruped crawler to a frog-like swimmer within 0.2 s. Aside from fully soft-bodied robot, soft materials can be employed as functional elements in robot with rigid support. This strategy facilitates the realization of large-scale amphibious robots, such as a bioinspired robotic turtle.^[87] Similarly, inspired by seal locomotion, a soft amphibious robot made of SMA-based actuators was proposed (Figure 6c).^[100] To replicate seal locomotion, two types of SMA-based soft actuators, a backbone unit integrating body and tail segments for primary propulsion and support units providing steering assistance, are utilized. Terrestrial crawling is achieved through antagonistic body-tail undulation which enables two-anchor kinematics, while aquatic propulsion relies on tail oscillation with static body posture.

Given the persistent technical challenges in achieving stable flight motion for soft robots, transitions within aerial environments remain a notable unexplored frontier in contrast with aquatic-terrestrial transitions. Micro flapping-wing robots actuated by smart materials provide a promising avenue for flight modality exploration.^[59] When such small-scale robots transition between aquatic and aerial media, interfacial phenomena must be addressed. An insect-scale flapping-wing robot overcomes air-water interfacial tension via bioinspired actuation and electrochemical phase-transition (Figure 6d).^[101] Its symmetric split-body design integrates a central gas collection chamber with buoyancy triggers, four titanium balance beams exploiting surface tension, and integrated electrolytic plates with a sparker. The water-to-air transition involves electrolytic gas generation for gradually lifting the robot out of water followed by spark-ignited combustion achieving takeoff.

Flying robots are versatile for obstacle avoidance, but they require substantial power to maintain aerial flight, making energy consumption and endurance persistent challenges. Compared to flight, terrestrial locomotion is more efficient despite being constrained by spatial limitations. Therefore, the incorporation of terrestrial locomotion to achieve intermittent flight offers a viable solution to the endurance problem. A subgram DEA-driven microrobot integrates flapping-wing propulsion and passive telescopic legs to enable terrestrial-aerial locomotion (Figure 6e).^[102] Its two-phase transition cycle combines a stance phase where legs store >80% impact energy and an aerial phase using high-frequency flapping to compensate energy loss while controlling altitude/attitude. This design enables seamless transition between ballistic hopping and controlled flight, reducing power consumption by 64% compared to pure flight. As validated in preceding sections, morphological reconfiguration provides an effective approach to perform multimodal locomotion in different environments. To enable efficient ground-air transition, a shape-morphing metamaterial functions as an essential component of soft robotic drones (Figure 6f).^[103] Composed of low-melting-point alloy endoskeletons, liquid metal heaters, and kirigami elastomers, it leverages kirigami's nonlinear deformation to induce complex morphologies. The shapes are fixed via plasticity and phases change of alloys, while liquid metal triggers reversible transitions. Integrated with motors, the robot can autonomously morph from a wheeled vehicle to a

quadrotor. Cross-domain multimodal soft robots represent a paradigm in adaptive machinery, enabling seamless transition between disparate environments through bioinspired design, which will revolutionize exploration, monitoring, and intervention in extreme terrestrial-aquatic-aerial domains.

4.2. Surface Adaptation

In confined-space operations such as aircraft cavity inspection, robots must achieve continuous locomotion transitions across diverse surfaces (e.g., planar, vertical, and inverted surfaces). This necessitates dynamic mode shift from terrestrial crawling/rolling to antigravity climbing for robots. Resolving such adaptive transitions on complex curved surfaces to enable efficient traversal poses a central challenge in designing these robotic systems. Contemporary research identifies two primary strategies for surface transition: active adhesion-based climbing and passive climbing enabled by microstructures.

Suction cup adhesion represents a prevalent implementation of active attachment mechanisms. As a typical example, a soft crawling-climbing robot achieves multimodal locomotion through synchronized body deformation and friction control (Figure 7a).^[104] The robot is composed of pneumatic artificial muscles for inchworm-like motion and suction cups for adhesion. During surface transitions, asymmetric actuation lifts the head while suction cups anchor to vertical surfaces. The system demonstrates confined-space navigation, aquatic mobility, and high load capacity. Similarly, an earthworm-inspired robot achieved adaptive climbing from horizontal plane up to 90° inclines via pneumatic muscles and electrostatic adhesion brakes (Figure 7b).^[105] Unlike multi-segment pneumatic systems, its dual electrostatic adhesion brakes enable extension, contraction, and bilateral bending modes for efficient climbing locomotion. Recently, a multimodal dual-segment soft robot has been developed capable of vertical climbing, ceiling crawling, and smooth inter-surface transitions, demonstrating the potential for deployment in real-world unstructured environments.^[106]

As another active attachment method, electrostatic adhesion demonstrates superior noise suppression capabilities compared to negative-pressure-based systems. However, its constrained payload capacity leads to primary application in small-scale robotic platforms. Voltage-driven laser-induced-graphene-LCE bilayer actuator enabling programmable 3D transformations and stiffness adjusting was developed for soft climbing robots (Figure 7c).^[44] The actuator is employed to develop morphable electroadhesive footpads adapting to curved surfaces and stiffness-tunable smart joints enabling gait switching. The robot achieves the transition from stepping to flipping via thermal joint control, allowing transitions between an 80° glass cylinder and a flat surface.

While the active control of functional feet provides a highly effective way for climbing, the increased number of actuators and control dimensionality adversely impact system integration. As an alternative strategy, passive microstructure-enabled surface transition is utilized in challenging climbing tasks. A piezoelectric-driven soft robot with bioinspired highly directional sliding-tuned footpads achieved robust surface adaptation, including roughness transition and angles transition (Figure 7d).^[107]

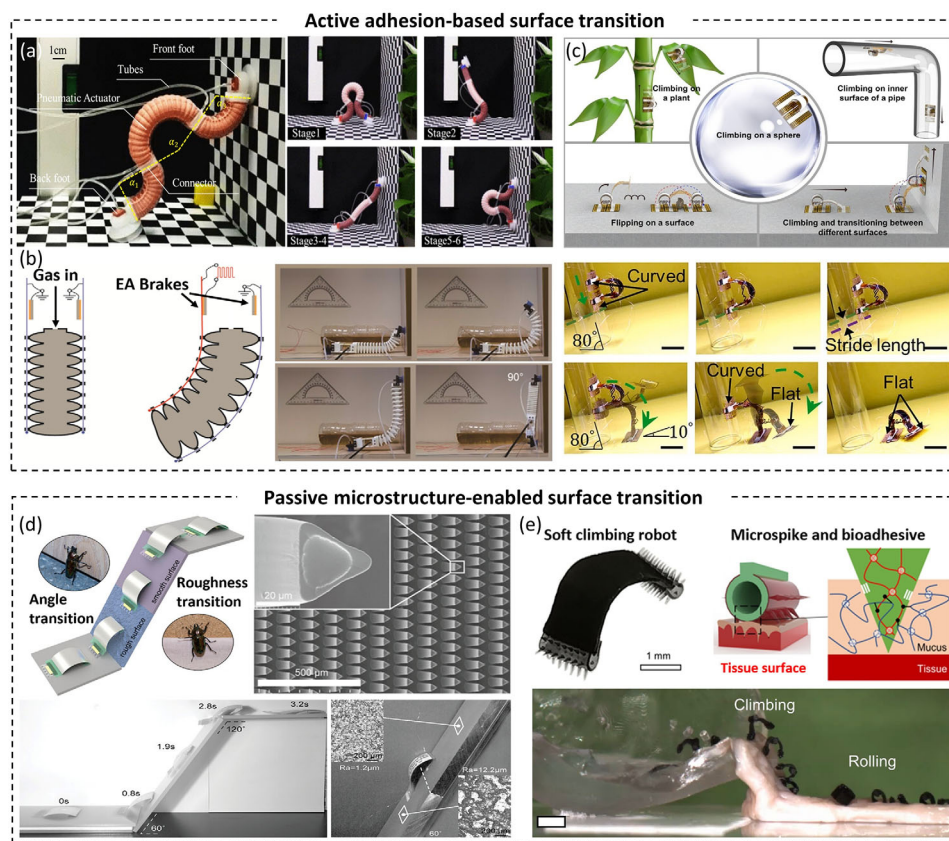


Figure 7. Adaptive multimodal locomotion transition on discontinuous surface. a) A soft crawling-climbing robot utilizing pneumatically actuated artificial muscles and negative pressure suckers to achieve surface transition. Reproduced with permission.^[104] Copyright 2022, IEEE. b) An earthworm-inspired robot capable of high-efficiency climbing locomotion featuring electrostatic adhesion-based strain-limiting layers with pneumatic actuators. Reproduced under terms of the CC-BY license.^[105] Copyright 2023, The Authors, published by Wiley. c) A soft microrobot capable of climbing and transitioning complex surfaces. Reproduced with permission.^[44] Copyright 2022, National Academy of Sciences. d) A piezoelectric-driven soft robot with bioinspired highly directional sliding-tuned footpads capable of robust surface adaptation. Reproduced with permission.^[107] Copyright 2023, Wiley. e) A magnetic soft millirobot that can climb 3D surfaces through microstructured footpad designs. Reproduced under terms of the CC-BY license.^[45] Copyright 2022, The Authors, published by AAAS.

Fabricated via inclined/soft lithography, these polydimethylsiloxane (PDMS) micropillars leverage directional contact and lift-drop mechanisms to enable extremely low forward friction for locomotion and high backward friction for slope stability. Another untethered soft millirobot climbs 3D surfaces through microstructured footpad designs under magnetic field (Figure 7e).^[45] The proposed peeling-and-loading mechanism utilizes both the soft-body deformation and whole-body motion of the robot to enable the adhesive control. Combining microspikes with bioadhesives, the robot achieves wet-surface locomotion (e.g., tissues), payload delivery, and pH-responsive drug release for biomedical applications.

4.3. Obstacle Negotiation

When navigating unstructured environments, robots often encounter obstacles (e.g., barriers, gaps, or stairs) that impede their current locomotion modality. Multimodal robots exhibit higher environmental adaptability than single-mode counterparts by dynamically changing locomotion strategies to fulfill obstacle-avoidance requirements. As a current research focus,

numerous robotic prototypes have been developed for obstacle negotiation, which can be categorized into bimodal transitional and multimodal synergistic types.

For bimodal transitional robots, jumping emerges as the predominant strategy employed for obstacle navigation due to its efficiency and feasibility.^[36,108] A biomimetic microrobot was developed capable of quadrupedal walking and impulsive jumping via a mantis shrimp-inspired catapult mechanism (Figure 8a).^[109] Torque reversal at linkage singularity rapidly releases elastic energy from SMA actuators, enabling directional jumping for obstacle clearance alongside agile walking. Additionally, a magnetically driven soft robot inspired by water striders leverages adaptive multimodal locomotion, including surface paddling, underwater swimming, terrestrial walking, and dynamic jumping, to overcome environmental barriers (Figure 8b).^[110] Composed of PDMS legs with NdFeB particles, the robot achieves in-flight maneuvers after jumping and payload-capable obstacle negotiation with grippers.

Another magnetoelastic soft robot employed crawling-to-tumbling transitions to overcome obstacles instead of jumping (Figure 8c).^[111] The NdFeB-Ecoflex body segments and Fe₃O₄ conical feet enable magnetic reconfiguration and low-friction

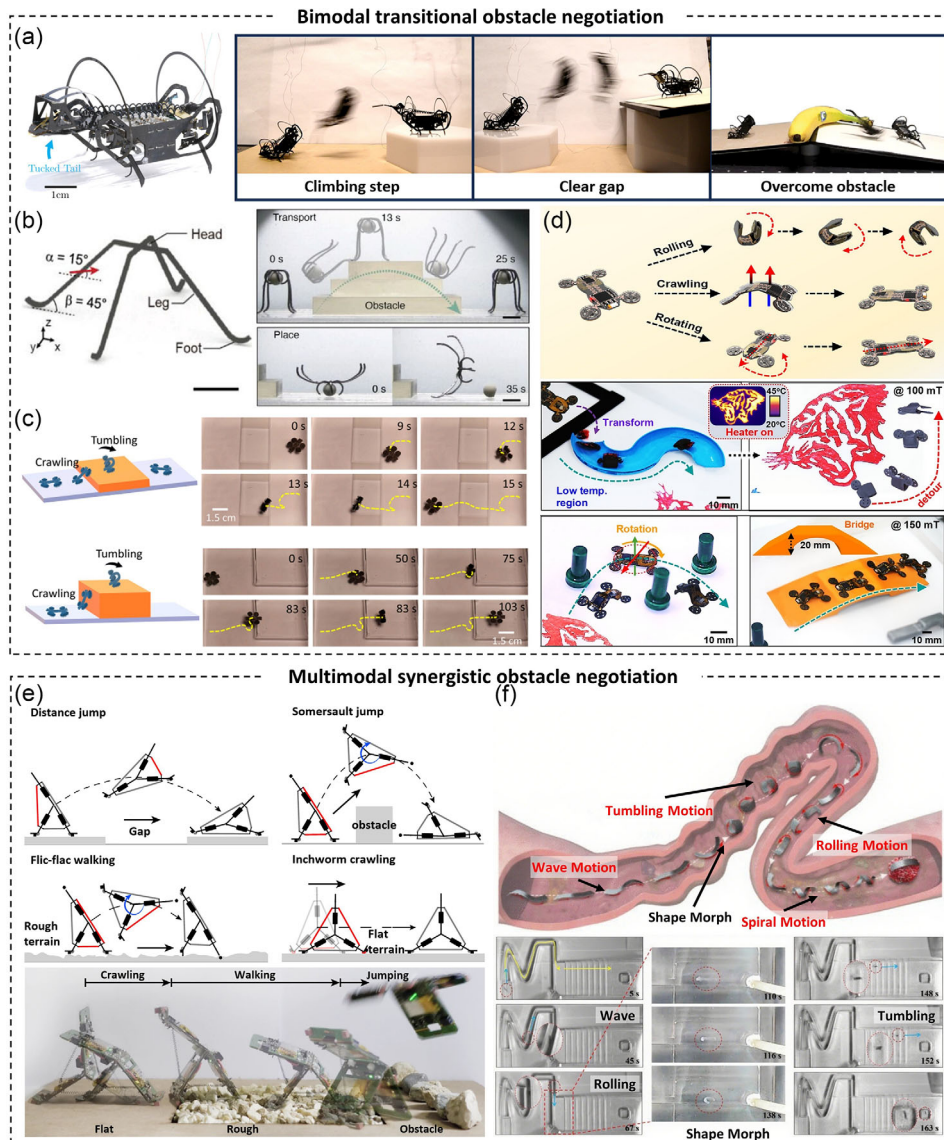


Figure 8. Adaptive multimodal locomotion transition for obstacle negotiation. a) A biomimetic microrobot capable of transitioning from quadrupedal walking to impulsive jumping to overcome obstacles. Reproduced with permission.^[109] Copyright 2025, AAAS. b) A magnetically driven soft robot inspired by water striders that can achieve payload-capable obstacle negotiation combining with functional grippers. Reproduced under terms of the CC-BY license.^[110] Copyright 2023, The Authors, published by Wiley. c) A magnetoelastic soft robot employing crawling-to-tumbling transitions to surmount barriers. Reproduced under terms of the CC-BY license.^[111] Copyright 2024, The Authors, published by AAAS. d) A reprogrammable magnetic soft robot utilizing reversible shape morphing and adaptive mode transitions to traverse pipes and narrow underpasses. Reproduced under terms of the CC-BY license.^[112] Copyright 2025, The Authors, published by Springer Nature. e) An insect-inspired millirobot with multiple specialized gaits generated by selective actuation of SMA actuators to overcome impassable terrain features. Reproduced with permission.^[113] Copyright 2019, Springer Nature. f) A soft thin-film millirobot enabling terrain-specific multimodal motions via dual-morphology and magnetic actuation. Reproduced with permission.^[114] Copyright 2025, IEEE.

motion. Upon encountering barriers, the robot anchors to obstacles, curls, and rolls to surmount them. For the scenario of narrow passages or geometrically complex tubes, planar crawling locomotion often fails to effective traversal. Consequently, the robot must either transition to locomotion modalities with reduced deformation or actively optimize its shape to minimize volumetric occupancy, thereby overcoming such constrained cases. A reprogrammable magnetic soft robot leverages

reversible shape morphing between fold and unfold states to navigate constrained environments (Figure 8d).^[112] While encountering S-shaped pipes and narrow underpasses, external magnetic fields trigger folding transformations that reduce the robot's profile, shifting the locomotion mode from crawling to rolling.

Confronting composite scenarios (e.g., combination of narrow channels and vertical barriers), reliance on binary locomotion

modality transitions proves insufficient, while robots capable of multimodal synergistic obstacle negotiation demonstrate superiority. An autonomous insect-inspired millirobot achieves adaptive obstacle traversal via a minimalistic Y-hinge design (Figure 8e).^[113] Selective SMA actuation triggers snap-through instability, generating five gaits: height jumping, distance jumping, somersault jumping, flic-flac walking, and inchworm crawling. When obstructed by impassable terrain features, the robot robustly transitions between modes, such as switching from crawling to flic-flac walking on rough surfaces or adopting somersault jumping to overcome obstacles. Another soft thin-film millirobot could also negotiate complex terrains via dual morphology and magnetic actuation (Figure 8f).^[114] Its magnetite-alginate hydrogel body switches between elongated and curled states via pH stimuli, enabling terrain-adaptive gaits: wave motion, rolling, tumbling, and spiral locomotion. Programmable magnetic fields orchestrate movements via knowledge graph-based modular control, validated in confined spaces, stair obstacles, and swine intestines. These multimodal soft robots, endowed with outstanding obstacle negotiation capabilities, execute efficient and resilient operations in unstructured complex environments, such as disaster reconnaissance and internal inspections of large-scale devices. Upon miniaturization, they manifest immense potential in medical domains like precise oncotargeting clearance and other micromanipulation procedures.

5. Challenges and Perspectives

Despite significant advancements in multimodal locomotion of soft robots, their overall performance still leaves room for improvement. One fundamental challenge lies in the efficient generation of multiple locomotion modes and their seamless transition. Current approaches predominantly rely on conceptual design and iterative experimental validation, which are often time-consuming and lacking in systematic design principles, thereby resulting in suboptimal performance.^[115] Addressing this requires unified physical modeling frameworks that incorporate multi-DOF actuation, complex soft-bodied structures, and multi-material distribution. Such frameworks should aim to accurately predict individual mode performance and capture critical transition conditions. Different multimodal locomotion strategies impose distinct requirements: the active control-based strategy requires accurate representation of spatiotemporal coordination across multiple actuators, the reconfiguration-based strategy may involve multistability analysis, and the environment-responsive strategy demands considering the interplay between body dynamics and external stimuli. These capabilities would enable programmable design and on-demand control of multimodal locomotion within a single robot. Moreover, design optimization guided by these models can further enhance overall locomotion performance.^[116] However, the persistent sim-to-real gap remains a bottleneck, as existing models and simulations often fail to fully capture the real-world interactions. Integrating machine learning with physics-based modeling can help compensate for model inaccuracies and uncertainties, offering a promising pathway to minimize this gap.

Another key challenge lies in sensing and control of multimodal soft robots. Due to their continuous and complex deformations, it is inherently difficult to model and estimate their internal

states (e.g., shape, pose, and contact forces) in real time. Addressing this challenge requires the development of embedded, distributed, high-density, low-latency, and interference-resilient proprioceptive systems. Emerging technologies such as optical fiber sensors, liquid metal sensors, and flexible capacitive or resistive strain sensor arrays offer promising avenues.^[117,118] The development of state estimation algorithms is equally important for inferring high-dimensional, time-varying states from noisy sensor data in real time.^[119] In the meantime, the inherent characteristics of soft robots, including high nonlinearities and time-varying dynamics, pose substantial challenges for accurate dynamic modeling. Consequently, robust control methods that can handle model uncertainty and environmental disturbances are crucial.^[120] Data-driven approaches, leveraging machine learning techniques such as neural networks and Gaussian processes, enable accurate modeling of soft robot dynamics that are difficult to capture analytically, offering strong potential for stable and robust multimodal locomotion under uncertain and dynamic conditions.^[121,122]

Although soft robots have demonstrated impressive multimodal locomotion capabilities in complex environments, their ability to perform practical tasks in real-world applications remains relatively limited. Some studies have endowed soft robots with basic operational capabilities, such as targeted cargo transport^[33,123,124] and controlled drug release.^[125–127] In addition, soft robots integrated with various types of sensors have been employed for detection tasks in confined environments, such as image capture,^[128,129] temperature sensing,^[112,130] and surface crack inspection.^[131] However, these functionalities are typically implemented in isolation, with most systems supporting only a single prescribed task. Beyond experimental or proof-of-concept demonstrations, multimodal locomotion of soft robots holds promise for broader and more impactful domains, such as minimally invasive surgery and exploration under extreme conditions (e.g., deep-sea or planetary environments), which are receiving increasing attention in current research.^[132–135] A critical challenge is to tightly integrate multiple functionalities, including actuation, power supply, sensing, and control,^[136,137] necessitating advances in soft materials, manufacturing techniques, and embedded system design. Future research should also address long-term durability and material lifecycle, particularly under repeated operation in harsh or unpredictable conditions.

Realizing practical applications in real-world scenarios also demands improvements in autonomy. To operate autonomously in unknown and dynamic environments, soft robots must be capable of making intelligent decisions, including real-time motion planning and optimal mode selection. Addressing this need requires the continued integration of advanced artificial intelligence techniques, such as online learning, adaptive control, and reinforcement learning.^[138] In particular, reinforcement learning shows great potential for enabling soft robots to autonomously discover novel locomotion gaits, optimize transition strategies, and adapt mode selection in response to dynamic and unpredictable environments. For instance, a recent study has employed reinforcement learning to enhance contact-aware control for a soft snake robot navigating obstacle-rich environments, demonstrating both feasibility and promising future of reinforcement learning in soft robotics.^[139] Equally important is the development of multimodal exteroceptive systems capable

of robustly detecting terrain geometry and robot-environment interaction states, providing essential inputs for decision-making and control. In parallel, an increasingly promising direction is the incorporation of autonomous physical intelligence, as exemplified by the environment-responsive strategy, enabling soft robots to exhibit intrinsically adaptive behavior by leveraging material properties and structural morphology and thereby minimizing reliance on complex sensing and control systems.^[95,140]

Acknowledgements

Z.Y., H.J., and K.H. contributed equally to this work. This work was supported in part by the National Natural Science Foundation of China under Grant T2293725 and Grant 52025057 and in part by the National Key Research and Development Program of China under Grant 2023YFB4706500.

Conflict of Interest

The authors declare no conflict of interest.

Keywords

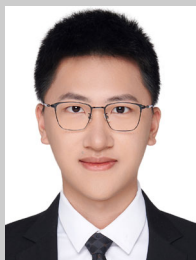
multi-environment adaptability, multimodal locomotion, soft robots

Received: July 15, 2025
Revised: September 1, 2025
Published online:

- [1] R. J. Lock, S. C. Burgess, R. Vaidyanathan, *Bioinspiration Biomimetics* **2013**, *9*, 011001.
- [2] D. Rus, M. T. Tolley, *Nature* **2015**, *521*, 467.
- [3] C. Laschi, B. Mazzolai, M. Cianchetti, *Sci. Rob.* **2016**, *1*, eaah3690.
- [4] S. Kim, C. Laschi, B. Trimmer, *Trends Biotechnol.* **2013**, *31*, 287.
- [5] R. F. Shepherd, F. Ilievski, W. Choi, S. A. Morin, A. A. Stokes, A. D. Mazzeo, X. Chen, M. Wang, G. M. Whitesides, *Proc. Natl. Acad. Sci.* **2011**, *108*, 20400.
- [6] C. D. Onal, D. Rus, *Bioinspiration Biomimetics* **2013**, *8*, 026003.
- [7] W. Wang, J.-Y. Lee, H. Rodrigue, S.-H. Song, W.-S. Chu, S.-H. Ahn, *Bioinspiration Biomimetics* **2014**, *9*, 046006.
- [8] T. Umedachi, V. Vikas, B. A. Trimmer, *Bioinspiration Biomimetics* **2016**, *11*, 025001.
- [9] H. Godaba, J. Li, Y. Wang, J. Zhu, *IEEE Rob. Autom. Lett.* **2016**, *1*, 624.
- [10] M. Pan, M. Liu, J. Lei, Y. Wang, C. Linghu, C. Bowen, K. J. Hsia, *Adv. Sci.* **2025**, *12*, 2416764.
- [11] Z. Yu, A. Duan, Z. Zhu, W. Zhang, *Sustainable Mater. Technol.* **2024**, *40*, e00930.
- [12] S. Chen, Y. Cao, M. Sarparast, H. Yuan, L. Dong, X. Tan, C. Cao, *Adv. Mater. Technol.* **2020**, *5*, 1900837.
- [13] Z. Ye, L. Zheng, W. Chen, B. Wang, L. Zhang, *Adv. Mater. Technol.* **2024**, *9*, 2301862.
- [14] Y. Sun, A. Abudula, H. Yang, S.-S. Chiang, Z. Wan, S. Ozel, R. Hall, E. Skorina, M. Luo, C. D. Onal, *Curr. Rob. Rep.* **2021**, *2*, 371.
- [15] M. Calisti, G. Picardi, C. Laschi, *J. R. Soc. Interface* **2017**, *14*, 20170101.
- [16] D. R. Yao, I. Kim, S. Yin, W. Gao, *Adv. Mater.* **2024**, *36*, 2308829.
- [17] C. S. X. Ng, M. W. M. Tan, C. Xu, Z. Yang, P. S. Lee, G. Z. Lum, *Adv. Mater.* **2021**, *33*, 2003558.
- [18] B. A. Trimmer, A. E. Takesian, B. M. Sweet, in *7th Int. Symp. on Technology and the Mine Problem*, Naval Postgraduate School, Monterey, CA **2006**, pp. 1–10.
- [19] J. Z. Ge, A. A. Calderón, L. Chang, N. O. Pérez-Arancibia, *Bioinspiration Biomimetics* **2019**, *14*, 036004.
- [20] P. Zhu, K. Shang, Y. Huang, Z. Jiang, J. Zhou, X. Lu, T. Yang, *Adv. Intell. Syst.* **2024**, *6*, 2300466.
- [21] S. Seok, C. D. Onal, K.-J. Cho, R. J. Wood, D. Rus, S. Kim, *IEEE/ASME Trans. Mechatron.* **2013**, *18*, 1485.
- [22] J. Liu, P. Li, Z. Huang, H. Liu, T. Huang, *Cyborg Bionic Syst.* **2025**, *6*, 0204.
- [23] C. Branyan, C. Fleming, J. Remaley, A. Kothari, K. Tumer, R. L. Hatton, Y. Mengüç, in *2017 IEEE Int. Conf. on Robotics and Biomimetics (ROBIO)*, IEEE, Piscataway, NJ **2017**, pp. 282–289, <https://doi.org/10.1109/ROBIO.2017.8324431>.
- [24] A. Rafsanjani, Y. Zhang, B. Liu, S. M. Rubinstein, K. Bertoldi, *Sci. Rob.* **2018**, *3*, eaar7555.
- [25] J. Tirado, A. Parvaresh, B. Seyidoğlu, D. A. Bedford, J. Jørgensen, A. Rafsanjani, *Cyborg Bionic Syst.* **2025**, *6*, 0301.
- [26] T. D. Ta, T. Umedachi, Y. Kawahara, in *2018 IEEE Int. Conf. on Robotics and Automation (ICRA)*, IEEE, Piscataway, NJ **2018**, pp. 6779–6785, <https://doi.org/10.1109/ICRA.2018.8463177>.
- [27] M. T. Tolley, R. F. Shepherd, B. Mosadegh, K. C. Galloway, M. Wehner, M. Karpelson, R. J. Wood, G. M. Whitesides, *Soft Rob.* **2014**, *1*, 213.
- [28] L. C. van Laake, J. de Vries, S. M. Kani, J. T. B. Overvelde, *Matter* **2022**, *5*, 2898.
- [29] Y. Li, Y. Chen, T. Ren, Y. Li, S. Choi, *Soft Rob.* **2018**, *5*, 567.
- [30] Z. Yuan, J. Li, L. Liu, X. Zhu, W. Wang, M. D. Dickey, G. Z. Lum, P. Chirarattananon, J. Luo, R. Chen, *IEEE Trans. Rob.* **2025**, *41*, 2894.
- [31] X. Yang, L. Chang, N. O. Pérez-Arancibia, *Sci. Rob.* **2020**, *5*, eaba0015.
- [32] H. Zeng, P. Wasylczyk, C. Parmeggiani, D. Martella, M. Burresi, D. S. Wiersma, *Adv. Mater.* **2015**, *27*, 3883.
- [33] Z. Li, Z. Ye, L. Han, Q. Fan, C. Wu, D. Ding, H. L. Xin, N. V. Myung, Y. Yin, *Adv. Mater.* **2021**, *33*, 2006367.
- [34] J. Zhao, J. Zhang, D. McCoul, Z. Hao, S. Wang, X. Wang, B. Huang, L. Sun, *Soft Rob.* **2019**, *6*, 713.
- [35] W. Feng, L. Sun, Z. Jin, L. Chen, Y. Liu, H. Xu, C. Wang, *Nat. Commun.* **2024**, *15*, 4222.
- [36] J. Yang, J. Zhou, F. Xu, H. Wang, *Soft Rob.* **2025**, *12*, 387.
- [37] W. Mu, M. Li, E. Chen, Y. Yang, J. Yin, X. Tao, G. Liu, R. Yin, *Adv. Funct. Mater.* **2023**, *33*, 2300516.
- [38] T. Park, Y. Cha, *Sci. Rep.* **2019**, *9*, 14700.
- [39] Y. Wu, J. K. Yim, J. Liang, Z. Shao, M. Qi, J. Zhong, Z. Luo, X. Yan, M. Zhang, X. Wang, R. S. Fearing, R. J. Full, L. Lin, *Sci. Rob.* **2019**, *4*, eaax1594.
- [40] G. Mao, D. Schiller, D. Danninger, B. Hailegnaw, F. Hartmann, T. Stockinger, M. Drack, N. Arnold, M. Kaltenbrunner, *Nat. Commun.* **2022**, *13*, 4456.
- [41] G. Gu, J. Zou, R. Zhao, X. Zhao, X. Zhu, *Sci. Rob.* **2018**, *3*, eaat2874.
- [42] T. Hu, X. Lu, J. Liu, *Adv. Intell. Syst.* **2023**, *5*, 2200209.
- [43] W.-K. Lee, D. J. Preston, M. P. Nemitz, A. Nagarkar, A. K. MacKeith, B. Gorissen, N. Vasios, V. Sanchez, K. Bertoldi, L. Mahadevan, G. M. Whitesides, *Sci. Rob.* **2022**, *7*, eabg5812.
- [44] W. Pang, S. Xu, J. Wu, R. Bo, T. Jin, Y. Xiao, Z. Liu, F. Zhang, X. Cheng, K. Bai, H. Song, Z. Xue, L. Wen, Y. Zhang, *Proc. Natl. Acad. Sci.* **2022**, *119*, e2215028119.
- [45] Y. Wu, X. Dong, J. Kim, C. Wang, M. Sitti, *Sci. Adv.* **2022**, *8*, eabn3431.
- [46] H.-T. Lin, G. G. Leisk, B. Trimmer, *Bioinspiration Biomimetics* **2011**, *6*, 026007.
- [47] A. Kotikian, C. McMahan, E. C. Davidson, J. M. Muhammad, R. D. Weeks, C. Daraio, J. A. Lewis, *Sci. Rob.* **2019**, *4*, eaax7044.
- [48] W.-B. Li, W.-M. Zhang, Q.-H. Gao, Q. Guo, S. Wu, H.-X. Zou, Z.-K. Peng, G. Meng, *Soft Rob.* **2021**, *8*, 611.
- [49] Y. Zhao, Y. Chi, Y. Hong, Y. Li, S. Yang, J. Yin, *Proc. Natl. Acad. Sci.* **2022**, *119*, e2200265119.

- [50] P. Yang, Y. Mao, H. Liu, L. Gao, F. Huang, F. Dang, *Soft Robotics*, ahead of print **2024**, <https://doi.org/10.1089/soro.2024.0115>.
- [51] Y. B. Kim, S. Yang, D. S. Kim, *Adv. Sci.* **2024**, *11*, 2308350.
- [52] C. Xu, J. Ma, L. Fu, X. Liu, L. Zhang, Y. Chen, *Adv. Sci.* **2025**, *12*, 2500577.
- [53] N. W. Bartlett, M. T. Tolley, J. T. B. Overvelde, J. C. Weaver, B. Mosadegh, K. Bertoldi, G. M. Whitesides, R. J. Wood, *Science* **2015**, *349*, 161.
- [54] C. A. Aubin, R. H. Heisser, O. Peretz, J. Timko, J. Lo, E. F. Helbling, S. Sobhani, A. D. Gat, R. F. Shepherd, *Science* **2023**, *381*, 1212.
- [55] R. Chen, Z. Yuan, J. Guo, L. Bai, X. Zhu, F. Liu, H. Pu, L. Xin, Y. Peng, J. Luo, L. Wen, Y. Sun, *Nat. Commun.* **2021**, *12*, 7028.
- [56] R. Chen, X. Zhu, Z. Yuan, H. Pu, J. Luo, Y. Sun, *IEEE Trans. Rob.* **2024**, *40*, 2149.
- [57] Q. Wang, X. Tian, D. Li, *Smart Mater. Struct.* **2021**, *30*, 085038.
- [58] J.-S. Koh, E. Yang, G.-P. Jung, S.-P. Jung, J. H. Son, S.-I. Lee, P. G. Jablonski, R. J. Wood, H.-Y. Kim, K.-J. Cho, *Science* **2015**, *349*, 517.
- [59] K. Y. Ma, P. Chirarattananon, S. B. Fuller, R. J. Wood, *Science* **2013**, *340*, 603.
- [60] A. Ramezani, S.-J. Chung, S. Hutchinson, *Sci. Rob.* **2017**, *2*, eaal2505.
- [61] Y.-W. Chin, J. M. Kok, Y.-Q. Zhu, W.-L. Chan, J. S. Chahl, B. C. Khoo, G.-K. Lau, *Sci. Rob.* **2020**, *5*, eaba2386.
- [62] Y. Chen, H. Zhao, J. Mao, P. Chirarattananon, E. F. Helbling, N. P. Hyun, D. R. Clarke, R. J. Wood, *Nature* **2019**, *575*, 324.
- [63] Z. Ren, S. Kim, X. Ji, W. Zhu, F. Niroui, J. Kong, Y. Chen, *Adv. Mater.* **2022**, *34*, 2106757.
- [64] E. Chang, L. Y. Matloff, A. K. Stowers, D. Lentink, *Sci. Rob.* **2020**, *5*, eaay1246.
- [65] E. Ajanic, M. Feroskhan, S. Mintchev, F. Noca, D. Floreano, *Sci. Rob.* **2020**, *5*, eaab2897.
- [66] B. Jenett, S. Calisch, D. Cellucci, N. Cramer, N. Gershenfeld, S. Swei, K. C. Cheung, *Soft Rob.* **2017**, *4*, 33.
- [67] C. Christianson, N. N. Goldberg, D. D. Deheyn, S. Cai, M. T. Tolley, *Sci. Rob.* **2018**, *3*, eaat1893.
- [68] H. Shahsavani, A. Aghakhani, H. Zeng, Y. Guo, Z. S. Davidson, A. Priimagi, M. Sitti, *Proc. Natl. Acad. Sci.* **2020**, *117*, 5125.
- [69] H.-W. Huang, F. E. Uslu, P. Katsamba, E. Lauga, M. S. Sakar, B. J. Nelson, *Sci. Adv.* **2019**, *5*, eaau1532.
- [70] T. Xu, J. Yu, C.-I. Vong, B. Wang, X. Wu, L. Zhang, *IEEE/ASME Trans. Mechatron.* **2019**, *24*, 924.
- [71] T. Li, G. Li, Y. Liang, T. Cheng, J. Dai, X. Yang, B. Liu, Z. Zeng, Z. Huang, Y. Luo, T. Xie, W. Yang, *Sci. Adv.* **2017**, *3*, e1602045.
- [72] G. Li, X. Chen, F. Zhou, Y. Liang, Y. Xiao, X. Cao, Z. Zhang, M. Zhang, B. Wu, S. Yin, Y. Xu, H. Fan, Z. Chen, W. Song, W. Yang, B. Pan, J. Hou, W. Zou, S. He, X. Yang, G. Mao, Z. Jia, H. Zhou, T. Li, S. Qu, Z. Xu, Z. Huang, Y. Luo, T. Xie, J. Gu, et al., *Nature* **2021**, *597*, 66.
- [73] X. Jia, Z. Chen, A. Riedel, T. Si, W. R. Hamel, M. Zhang, *IEEE Trans. Rob.* **2015**, *31*, 1432.
- [74] Z. Ren, W. Hu, X. Dong, M. Sitti, *Nat. Commun.* **2019**, *10*, 2703.
- [75] Z. Li, N. V. Myung, Y. Yin, *Sci. Rob.* **2021**, *6*, eabi4523.
- [76] M. A. Robertson, J. Paik, *Sci. Rob.* **2017**, *2*, eaan6357.
- [77] Q. Fang, J. Zhang, Y. He, N. Zheng, Y. Wang, R. Xiong, Z. Gong, H. Lu, *Research* **2024**, *7*, 0357.
- [78] Q. Yu, N. Gravish, *Soft Rob.* **2024**, *11*, 21.
- [79] Y. Kim, X. Zhao, *Chem. Rev.* **2022**, *122*, 5317.
- [80] Y.-Y. Xiao, Z.-C. Jiang, Y. Zhao, *Adv. Intell. Syst.* **2020**, *2*, 2000148.
- [81] W. Hu, G. Z. Lum, M. Mastrangeli, M. Sitti, *Nature* **2018**, *554*, 81.
- [82] T. Wang, Y. Wu, E. Yildiz, S. Kanyas, M. Sitti, *Nat. Rev. Bioeng.* **2024**, *2*, 470.
- [83] Y. Tang, F. Pan, L. Qin, Y. Yu, *Adv. Funct. Mater.* **2025**, 2506987, <https://doi.org/10.1002/adfm.202506987>.
- [84] D. Wang, B. Zhao, X. Li, L. Dong, M. Zhang, J. Zou, G. Gu, *Nat. Commun.* **2023**, *14*, 5067.
- [85] D. S. Shah, J. P. Powers, L. G. Tilton, S. Kriegman, J. Bongard, R. Kramer-Bottiglio, *Nat. Mach. Intell.* **2021**, *3*, 51.
- [86] M. Polzin, Q. Guan, J. Hughes, *Sci. Rob.* **2025**, *10*, eadp6419.
- [87] R. Baines, S. K. Patiballa, J. Booth, L. Ramirez, T. Sipple, A. Garcia, F. Fish, R. Kramer-Bottiglio, *Nature* **2022**, *610*, 283.
- [88] S. Xu, X. Hu, R. Yang, C. Zang, L. Li, Y. Xiao, W. Liu, B. Tian, W. Pang, R. Bo, Q. Liu, Y. Yang, Y. Lai, J. Wu, H. Zhao, L. Wen, Y. Zhang, *Nat. Mach. Intell.* **2025**, *7*, 703.
- [89] F. Pan, J. Liu, Z. Zuo, X. He, Z. Shao, J. Chen, H. Wang, Q. Zhang, F. Yuan, B. Chen, T. Jin, L. He, Y. Wang, K. Zhang, X. Ding, T. Li, L. Wen, *Sci. Rob.* **2025**, *10*, eadp7821.
- [90] J.-S. Park, K. Ki, A. Lee, J.-Y. Sun, H.-Y. Kim, *Cell Rep. Phys. Sci.* **2025**, *6*, 102448.
- [91] Q. Ze, S. Wu, J. Dai, S. Leanza, G. Ikeda, P. C. Yang, G. Iaccarino, R. R. Zhao, *Nat. Commun.* **2022**, *13*, 3118.
- [92] X. Zhou, G. Chen, B. Jin, H. Feng, Z. Chen, M. Fang, B. Yang, R. Xiao, T. Xie, N. Zheng, *Adv. Sci.* **2024**, *11*, 2402358.
- [93] A. Comoretto, H. A. H. Schomaker, J. T. B. Overvelde, *Science* **2025**, *388*, 610.
- [94] Z. Zheng, J. Han, S. O. Demir, H. Wang, W. Jiang, H. Liu, M. Sitti, *Adv. Sci.* **2023**, *10*, 2302409.
- [95] C. Chen, P. Shi, Z. Liu, S. Duan, M. Si, C. Zhang, Y. Du, Y. Yan, T. J. White, R. Kramer-Bottiglio, M. Sitti, T. Iwasaki, X. He, *Sci. Rob.* **2025**, *10*, eads1292.
- [96] X. Wang, S. Li, J.-C. Chang, J. Liu, D. Axinte, X. Dong, *Nat. Commun.* **2024**, *15*, 6296.
- [97] J. Che, X. Yang, J. Peng, J. Li, Z. Liu, M. Qi, *Nat. Commun.* **2025**, *16*, 3014.
- [98] F. Fang, J. Zhou, Y. Zhang, Y. Yi, Z. Huang, Y. Feng, K. Tao, W. Li, W. Zhang, *Cyborg Bionic Syst.* **2025**, *6*, 0253.
- [99] D. K. Patel, X. Huang, Y. Luo, M. Mungekar, M. K. Jawed, L. Yao, C. Majidi, *Adv. Mater. Technol.* **2023**, *8*, 2201259.
- [100] J. Hwang, W. D. Wang, *Adv. Mater. Technol.* **2022**, *7*, 2101153.
- [101] Y. Chen, H. Wang, E. F. Helbling, N. T. Jafferis, R. Zufferey, A. Ong, K. Ma, N. Gravish, P. Chirarattananon, M. Kovac, R. J. Wood, *Sci. Rob.* **2017**, *2*, eaao5619.
- [102] Y.-H. Hsiao, S. Bai, Z. Guan, S. Kim, Z. Ren, P. Chirarattananon, Y. Chen, *Sci. Adv.* **2025**, *11*, eadu4474.
- [103] D. Hwang, E. J. Barron, A. B. M. T. Haque, M. D. Bartlett, *Sci. Rob.* **2022**, *7*, eabg2171.
- [104] Y. Zhang, D. Yang, P. Yan, P. Zhou, J. Zou, G. Gu, *IEEE Trans. Rob.* **2022**, *38*, 1806.
- [105] Q. Xiong, B. W. K. Ang, T. Jin, J. W. Ambrose, R. C. H. Yeow, *Adv. Intell. Syst.* **2023**, *5*, 2200346.
- [106] R. Yuan, K. Huang, C. Ying, Y. Hu, Z. Yuan, F. Chen, *IEEE Rob. Autom. Lett.* **2025**, *10*, 10729.
- [107] M. Zheng, D. Wang, D. Zhu, S. Cao, X. Wang, M. Zhang, *Adv. Funct. Mater.* **2024**, *34*, 2308384.
- [108] M. Duduta, F. Berlinger, R. Nagpal, D. R. Clarke, R. J. Wood, F. Z. Temel, *IEEE Rob. Autom. Lett.* **2020**, *5*, 3868.
- [109] F. Ramirez Serrano, N. P. Hyun, E. Steinhardt, P.-L. Lechère, R. J. Wood, *Sci. Rob.* **2025**, *10*, eadp7854.
- [110] Y. Wang, X. Du, H. Zhang, Q. Zou, J. Law, J. Yu, *Adv. Sci.* **2023**, *10*, 2207493.
- [111] B. Wang, Y. Chen, Z. Ye, H. Yu, K. F. Chan, T. Xu, Z. Guo, W. Liu, L. Zhang, *Cyborg Bionic Syst.* **2024**, *5*, 0138.
- [112] S. Han, J.-W. Shin, J. H. Lee, B. Li, G.-J. Ko, T.-M. Jang, A. Dutta, W. B. Han, S. M. Yang, D.-J. Kim, H. Kang, J. H. Lim, C.-H. Eom, S. J. Choi, H. Cheng, S.-W. Hwang, *Nano Micro Lett.* **2025**, *17*, 152.
- [113] Z. Zhakypov, K. Mori, K. Hosoda, J. Paik, *Nature* **2019**, *571*, 381.

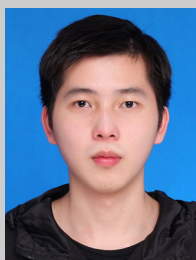
- [114] Z. Xin, S. Zhong, A. Wu, Z. Zheng, Q. Shi, Q. Huang, T. Fukuda, H. Wang, *IEEE Trans. Rob.* **2025**, *41*, 2662.
- [115] J. Pinskiar, D. Howard, *Adv. Intell. Syst.* **2022**, *4*, 2100086.
- [116] F. Chen, M. Y. Wang, *IEEE Rob. Autom. Mag.* **2020**, *27*, 27.
- [117] C. Hegde, J. Su, J. M. R. Tan, K. He, X. Chen, S. Magdassi, *ACS Nano* **2023**, *17*, 15277.
- [118] Q. Zhang, N. Li, Y. Song, C. Hua, T. Guan, Y. Ma, C. Cheng, J. Liu, *Adv. Rob. Res.* **2025**, 202500057, <https://doi.org/10.1002/adrr.202500057>.
- [119] J.-H. Lee, K. Cho, J.-K. Kim, *Adv. Mater.* **2024**, *36*, 2310505.
- [120] X. Huang, Z. Yuan, X. Yang, G. Gu, *IEEE Trans. Rob.* **2024**, *40*, 3565.
- [121] Z. Chen, F. Renda, A. Le Gall, L. Mocellin, M. Bernabei, T. Dangel, G. Ciuti, M. Cianchetti, C. Stefanini, *IEEE Trans. Autom. Sci. Eng.* **2025**, *22*, 2241.
- [122] J. Wang, A. Chortos, *Adv. Intell. Syst.* **2022**, *4*, 2100165.
- [123] X. Li, Z. Shang, Y. Wang, J. Liu, Y. Xie, J. Li, Y. Liu, W. Gan, *ACS Appl. Mater. Interfaces* **2023**, *15*, 28442.
- [124] Y. Cheng, K. H. Chan, X.-Q. Wang, T. Ding, T. Li, C. Zhang, W. Lu, Y. Zhou, G. W. Ho, *Adv. Funct. Mater.* **2021**, *31*, 2101825.
- [125] Q. Ze, S. Wu, J. Nishikawa, J. Dai, Y. Sun, S. Leanza, C. Zemelka, L. S. Novelino, G. H. Paulino, R. R. Zhao, *Sci. Adv.* **2022**, *8*, eabm7834.
- [126] Z. Yang, C. Xu, J. X. Lee, G. Z. Lum, *Adv. Mater.* **2024**, *36*, 2408750.
- [127] H. Li, S. Jiang, Q. Deng, W. Li, W. Zhang, H. Zhu, Z. Zhao, Y. Zhang, L. Wang, L. Xu, *Mater. Today* **2025**, *87*, 66.
- [128] T. T. Nguyen, D. Q. Nguyen, V. A. Ho, *IEEE Trans. Rob.* **2024**, *40*, 3933.
- [129] C. Tang, B. Du, S. Jiang, Q. Shao, X. Dong, X.-J. Liu, H. Zhao, *Sci. Rob.* **2022**, *7*, eabm8597.
- [130] Y. Dong, L. Wang, N. Xia, Z. Yang, C. Zhang, C. Pan, D. Jin, J. Zhang, C. Majidi, L. Zhang, *Sci. Adv.* **2022**, *8*, eabn8932.
- [131] P. Yang, B. Huang, D. McCoul, D. Xie, M. Li, J. Zhao, *Soft Rob.* **2023**, *10*, 280.
- [132] N. Ebrahimi, C. Bi, D. J. Cappelleri, G. Ciuti, A. T. Conn, D. Faivre, N. Habibi, A. Hošovský, V. Iacovacci, I. S. M. Khalil, V. Magdanz, S. Misra, C. Pawashe, R. Rashidifar, P. E. D. Soto-Rodriguez, Z. Fekete, A. Jafari, *Adv. Funct. Mater.* **2021**, *31*, 2005137.
- [133] J. Qu, Y. Xu, Z. Li, Z. Yu, B. Mao, Y. Wang, Z. Wang, Q. Fan, X. Qian, M. Zhang, M. Xu, B. Liang, H. Liu, X. Wang, X. Wang, T. Li, *Adv. Intell. Syst.* **2024**, *6*, 2300299.
- [134] G. Li, T.-W. Wong, B. Shih, C. Guo, L. Wang, J. Liu, T. Wang, X. Liu, J. Yan, B. Wu, F. Yu, Y. Chen, Y. Liang, Y. Xue, C. Wang, S. He, L. Wen, M. T. Tolley, A.-M. Zhang, C. Laschi, T. Li, *Nat. Commun.* **2023**, *14*, 7097.
- [135] Y. Zhang, P. Li, J. Quan, L. Li, G. Zhang, D. Zhou, *Adv. Intell. Syst.* **2023**, *5*, 2200071.
- [136] X.-Q. Wang, G. W. Ho, *Mater. Today* **2022**, *53*, 197.
- [137] S. I. Rich, R. J. Wood, C. Majidi, *Nat. Electron.* **2018**, *1*, 102.
- [138] H. Guo, F. Wu, Y. Qin, R. Li, K. Li, K. Li, *ACM Comput. Surv.* **2023**, *55*, 289:1.
- [139] X. Liu, C. D. Onal, J. Fu, *IEEE Trans. Rob.* **2025**, *41*, 1581.
- [140] V. G. Kortman, B. Mazzolai, A. Sakes, J. Jovanova, *Adv. Intell. Syst.* **2025**, *7*, 2400294.



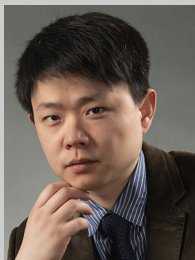
Zihao Yuan received the B.E. degree in mechanical engineering in 2022 from Shanghai Jiao Tong University, China. He is currently working toward the Ph.D. degree in mechanical engineering at Shanghai Jiao Tong University. His research interests include design and control of pneumatic soft robots and bioinspired soft robots.



Huangwei Ji completed his undergraduate studies at the Shanghai Jiao Tong University (B.Sc.), Shanghai, China. He is currently working toward the Ph.D. degree in mechanical engineering at Shanghai Jiao Tong University. His research interests include soft robotics and artificial muscles.



Kai Huang completed his undergraduate studies at the Shanghai Jiao Tong University (B.Sc.), Shanghai, China. He is currently working toward the Ph.D. degree in mechanical engineering at Shanghai Jiao Tong University. His research interests include modeling and control of soft robots.



Feifei Chen is currently a Tenured Associate Professor with the School of Mechanical Engineering, Shanghai Jiao Tong University, China. He received his B.E. degree in mechanical engineering from University of Science and Technology of China and the Ph.D. degree in mechanical engineering from the National University of Singapore, in 2013 and 2018, respectively. His research interests include design theories and methodologies for soft robotics.



Guoying Gu is currently a Distinguished Professor with the School of Mechanical Engineering, Shanghai Jiao Tong University, China. He received his B.E. degree (with honors) in electronic science and technology and the Ph.D. degree (with honors) in mechatronic engineering, from Shanghai Jiao Tong University, in 2006 and 2012, respectively. His research interests include soft robotics, bioinspired and wearable robots, smart materials sensing, actuation, and motion control. He has authored or coauthored more than 150 publications, which have appeared in Science Robotics, Nature Biomedical Engineering, Nature Reviews Materials, Nature Materials, Nature Communications, Science Advances, IEEE/ASME Transactions, Advanced Materials, Soft Robotics, etc.